A dissipative filter for DG with sub-cell discontinuity resolution

Konstantinos Panourgias

and

John Ekaterinaris

Embry-Riddle Aeronautical University

ERAU

Daytona Beach FL

AMS Seminar Series,
NASA Ames Research Center, Jan 11, 2016

ERAU

Outline of the Presentation

- Motivation and Objectives
- Numerical Method
- The dissipative filter
- Results for model problems
- Conclusions

Motivation and Objectives

- To develop a unified efficient approach for discontinuity capturing with higher-order (P2 or higher) DG discretizations in three-dimensional unstructured meshes

- To allow capabilities of using large cells and high order accuracy both at discontinuities (with sub-cell discontinuity resolution) and away from them in order to resolve smooth but complex flow features.

- To advance implicitly in time the full coupled system for chemically reactive flows

- To apply and demonstrate dynamic h/p refinement for time dependent complex three dimensional flow problems.

ERAU

DG discretization

$$\frac{\partial U}{\partial t} + div\,\bar{\bar{Q}} = S$$

- Weak form of the system

$$\int_{\Omega} \Phi \frac{\partial \boldsymbol{U}}{\partial t}\, d\Omega = \int_{\Omega} \nabla\Phi \cdot \boldsymbol{Q}(\boldsymbol{U},\nabla \boldsymbol{U})\, d\Omega - \int_{\partial\Omega} \Phi \boldsymbol{Q}(\boldsymbol{U},\nabla \boldsymbol{U}) \cdot \boldsymbol{n}\, dA + \int_{\Omega} \Phi \cdot \boldsymbol{S}(\boldsymbol{U})\, d\Omega$$

- Use the same polynomial spaces for weighting and expansion functions

- The approximate solution is $\boldsymbol{U}_h = \sum_i c_i \Phi_i$ and the discrete weak form becomes

$$\mathrm{M}\frac{\partial \mathbf{c}}{\partial t} = \int_{K} \nabla\Phi_i \cdot \boldsymbol{Q}(\boldsymbol{U}_h,\nabla \boldsymbol{U}_h)\, dK - \int_{S_K} \Phi_i \breve{\boldsymbol{Q}}(\boldsymbol{U}_h,\nabla \boldsymbol{U}_h) \cdot \boldsymbol{n}\, dS_K + \int_{K} \Phi_i \boldsymbol{S}(\boldsymbol{U}_h)\, dK$$

- Use the LLF or Roe's flux to evaluate the interface fluxes

LLF flux
$$\breve{\boldsymbol{Q}}(\boldsymbol{U}_h) = 0.5\left[\boldsymbol{Q}^{+}(\boldsymbol{U}_h)\cdot\boldsymbol{n} + \boldsymbol{Q}^{-}(\boldsymbol{U}_h)\cdot\boldsymbol{n} - \lambda_{\max}(\boldsymbol{U}_h^{-} - \boldsymbol{U}_h^{+})\right]$$

ERAU

DG discretization of the viscous terms

ERAU

- Define the auxiliary variable $\Theta = \nabla \mathbf{U}_f$ for the gradient of the state vector and discretize it in the same DG framework

$$\mathrm{M}\boldsymbol{c} = \int_{S_K} \Phi_i \breve{\boldsymbol{U}}_h \cdot \boldsymbol{n} dS_K - \int_K \nabla \Phi_i \cdot \boldsymbol{U}_h dK$$

- Use the LDG or the BR2 scheme to evaluate the numerical fluxes
- For the current computations we used the LDG method
- For arbitrary three dimensional meshes the BR2 scheme is more suitable because it yields more narrow stencils strictly confined to the immediate neighbors of an element

Fundamentals of TVB and TVD limiting

ERAU

- To eliminate oscillations at strong discontinuities of both the flow field and the electromagnetic field variable the following TVB limiter is used

$$\bar{m}(a_1, a_2, a_3) = \begin{cases} a_1 & \text{if } |a_1| \leq \wp L^2 \\ m(a_1, a_2, a_3) & \text{otherwise} \end{cases}$$

the parameter $\wp$ is an estimation of second order derivative of variable u and it is estimated by the Laplacian $\wp(u)$; $\nabla^2 u$ in the transformed space

- The TVB limiter is applied to the characteristic variables of the flow field
- TVB Limiting is performed in the transformed canonical space of cubic elements to the characteristic variables and the limited variables are transferred back to the physical domain using collapsed coordinates
- Limiting is applied for all variable at the end of each RK stage
- TVD limiting can be applied in the physical space it is more diffusive than the TVB limiter and the computational cost is not very low

Applications of the TVB and hierarchical limiters

Hierarchical Limiter

$$u_h^h = \sum_{i=0}^{26} c_i^h b_i^h$$

$$\begin{aligned}\widetilde{c_i^h} = m\big(c_i^h, &(\alpha_1/L)(c^h_{l,(i+1,j,k)} - c^h_{l,(i,j,k)}), (\alpha_1/L)(c^h_{l,(i,j,k)} - c^h_{l,(i-1,j,k)}),\\ &(\alpha_2/L)(c^h_{m,(i,j+1,k)} - c^h_{m,(i,j,k)}), (\alpha_2/L)(c^h_{m,(i,j,k)} - c^h_{m,(i,j-1,k)}),\\ &(\alpha_3/L)(c^h_{n,(i,j,k+1)} - c^h_{n,(i,j,k)}), (\alpha_3/L)(c^h_{n,(i,j,k)} - c^h_{n,(i-1,j,k-1)})\big)\end{aligned}$$

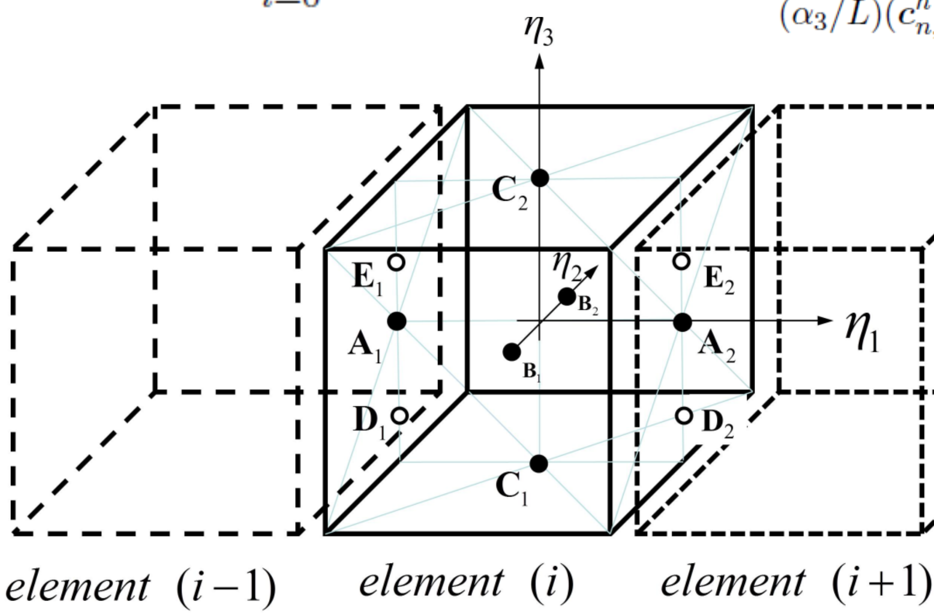

P1 Limiter

$$\overline{m}(a_1, a_2, \ldots, a_n) = \begin{cases} a_1 & \text{if } |a_1| \le ML^2_{x,y,z} + b, \\ m(a_1, a_2, \ldots, a_n) & \text{otherwise.} \end{cases}$$

$$\begin{aligned}u_h^h = c_0^h + c_1^h\eta_1 + c_2^h\eta_2 + c_3^h\eta_3\\ + c_4^h\eta_1\eta_2 + c_5^h\eta_1\eta_3 + c_6^h\eta_2\eta_3\\ + c_7^h\eta_1\eta_2\eta_3\end{aligned}$$

$$U_{A_1} = u^h(-1,0,0) - c_0^h = -c_1^h,$$

$$U_{A_2} = u^h(1,0,0) - c_0^h = c_1^h,$$

$$\widetilde{U}_{A_1} = -m(-U_{A_1}, c^h_{0,(i+1,j,k)} - c^h_{0,(i,j,k)}, c^h_{0,(i,j,k)} - c^h_{0,(i-1,j,k)}),$$

$$\widetilde{U}_{A_2} = m(U_{A_2}, c^h_{0,(i+1,j,k)} - c^h_{0,(i,j,k)}, c^h_{0,(i,j,k)} - c^h_{0,(i-1,j,k)}),$$

$$\widetilde{c}_1^h = \frac{\widetilde{U}_{A_2} - \widetilde{U}_{A_1}}{2}.$$

Adaptive mesh refinement with P1+TVB limiter for enhanced resolution of discontinuities and complex flow features

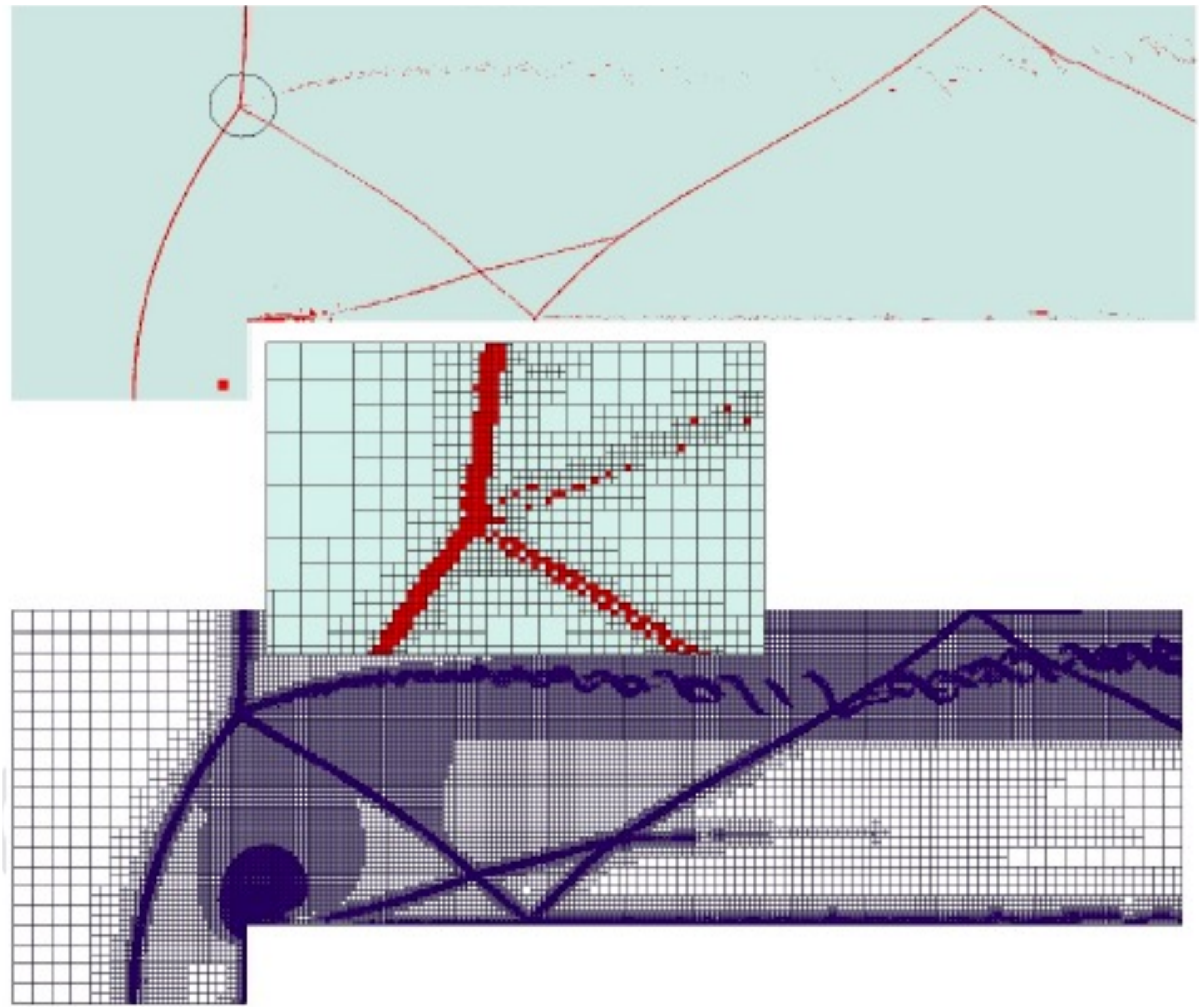

Adaptive mesh refinement and parallel efficiency

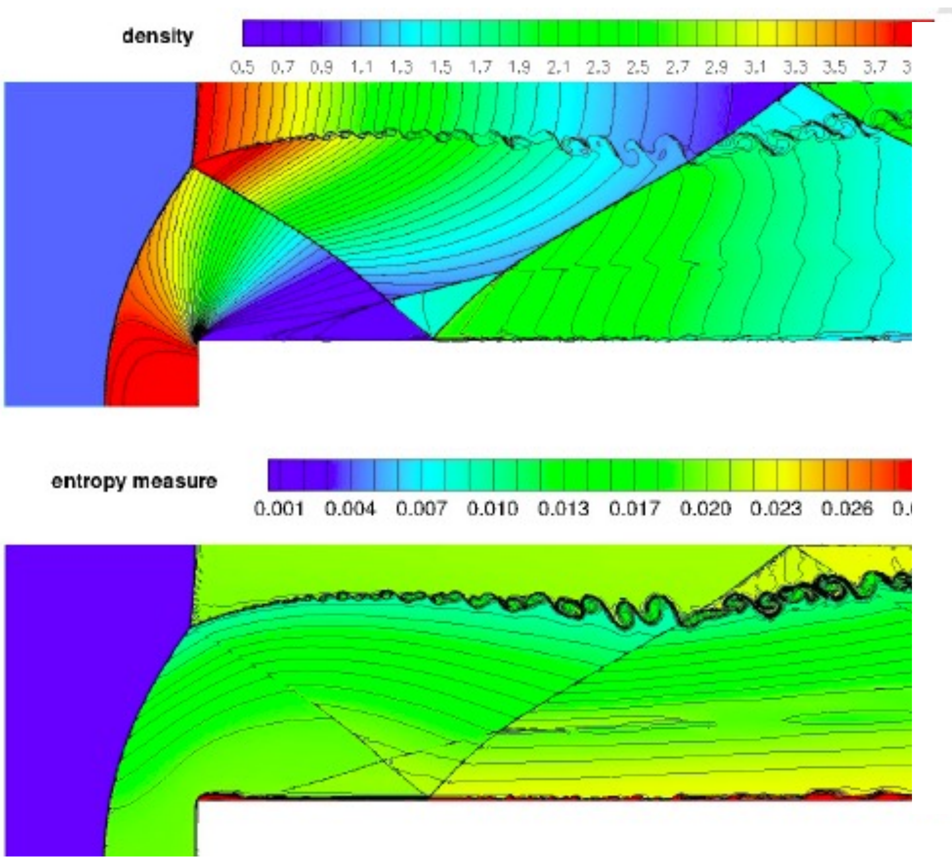

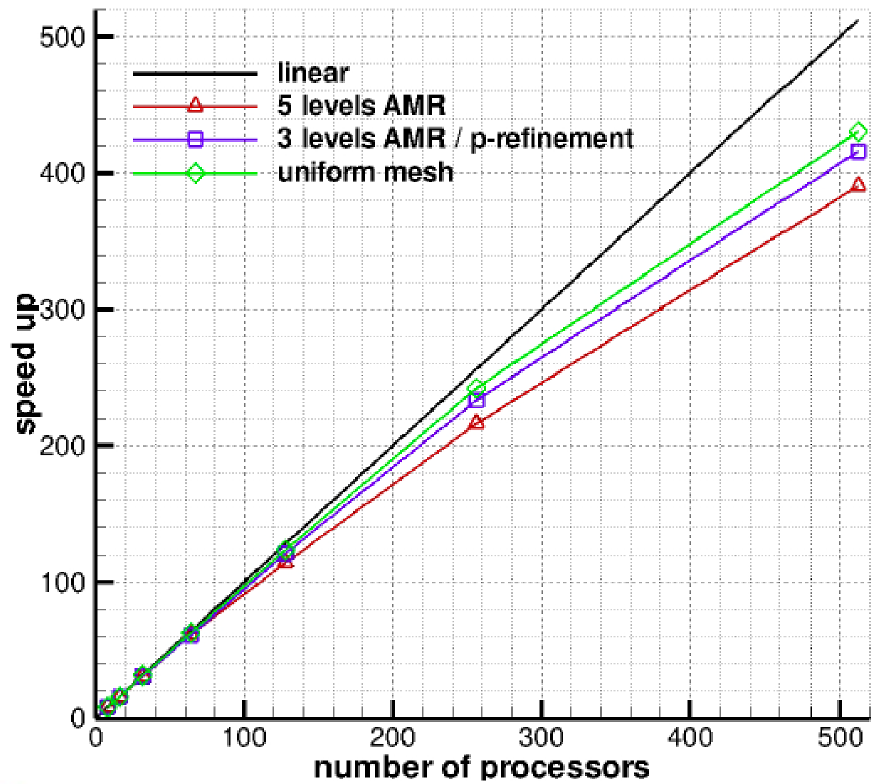

The dissipative filter for P1 or higher-order expansions

Let $\boldsymbol{LF_x}$ be the dissipative flux of the filter operator along the x direction with similar definitions for $\boldsymbol{LFy}$ and $\boldsymbol{LFz}$ along the other directions

$$\mathbf{LF}_x(F^*) = \frac{1}{\Delta x}\left[F^*_{i+1/2} - F^*_{i-1/2}\right]$$

$$\begin{aligned} U^{n+1} &= \hat{U}^{n+1} + (\Delta t)\left[\mathbf{LF}_x(F^*) + \mathbf{LF}_y(G^*) + \mathbf{LF}_z(H^*)\right] \\ &= \hat{U}^{n+1} + (\Delta t)\,\mathbf{LF} \end{aligned}$$

and in the finite element context

$$\int_{\Omega_{\mathrm{m}}} wU^{n+1} d\Omega_{\mathrm{m}} = \int_{\Omega_{\mathrm{m}}} wU^{n+1} d\Omega_{\mathrm{m}} + (\Delta t)\int_{\Omega_{\mathrm{m}}} w\,\mathbf{LF}\, d\Omega_{\mathrm{m}}$$

The filter dissipative fluxes

$$F^*_{i+1/2} = \frac{1}{2} R_{i+1/2}\, \Phi^*_{i+1/2}$$

$R_{i+1/2}$ are the right eigenvectors evaluated at Roe's averae state and the elements φ^* of the matrix $\Phi^*_{i+1/2}$ are given by

$$\varphi^*_{i+1/2} = \kappa\ \theta_{i+1/2}\ \varphi_{i+1/2}$$

the function $\kappa\ \theta_{i+1/2}$ plays the role of discontinuity detector

where $0.03 < \kappa < 2$

or it is evaluated based on the smothness of computed solution

and $\theta_{i+1/2}$ is evaluated as suggested by Yee

$$\theta_{i+1/2} = \max\left(\hat{\theta}_{i-m+1}, \ldots, \hat{\theta}_{i+m}\right) \quad \hat{\theta}_i = \left| \frac{\left|r_{i+1/2}\right| - \left|r_{i-1/2}\right|}{\left|r_{i+1/2}\right| + \left|r_{i-1/2}\right|} \right|^p$$

where $r_{i+1/2}$ are the elements of $R^{-1}{}_{i+1/2}\Delta U$

Application of the filter in 1D for P1, P2, and P3 expansions using information from neighboring elements

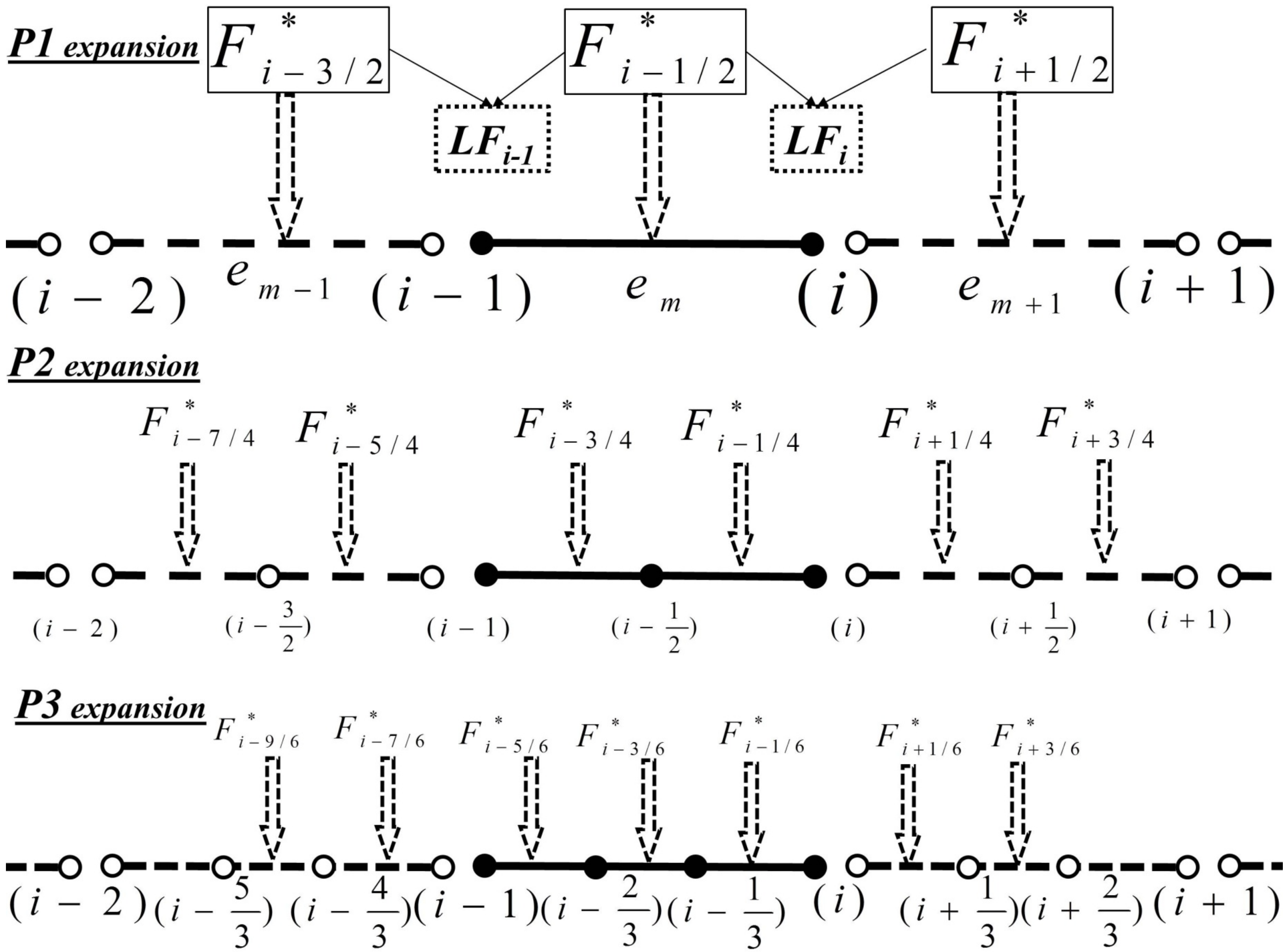

Application of the filter for quadrilateral elements

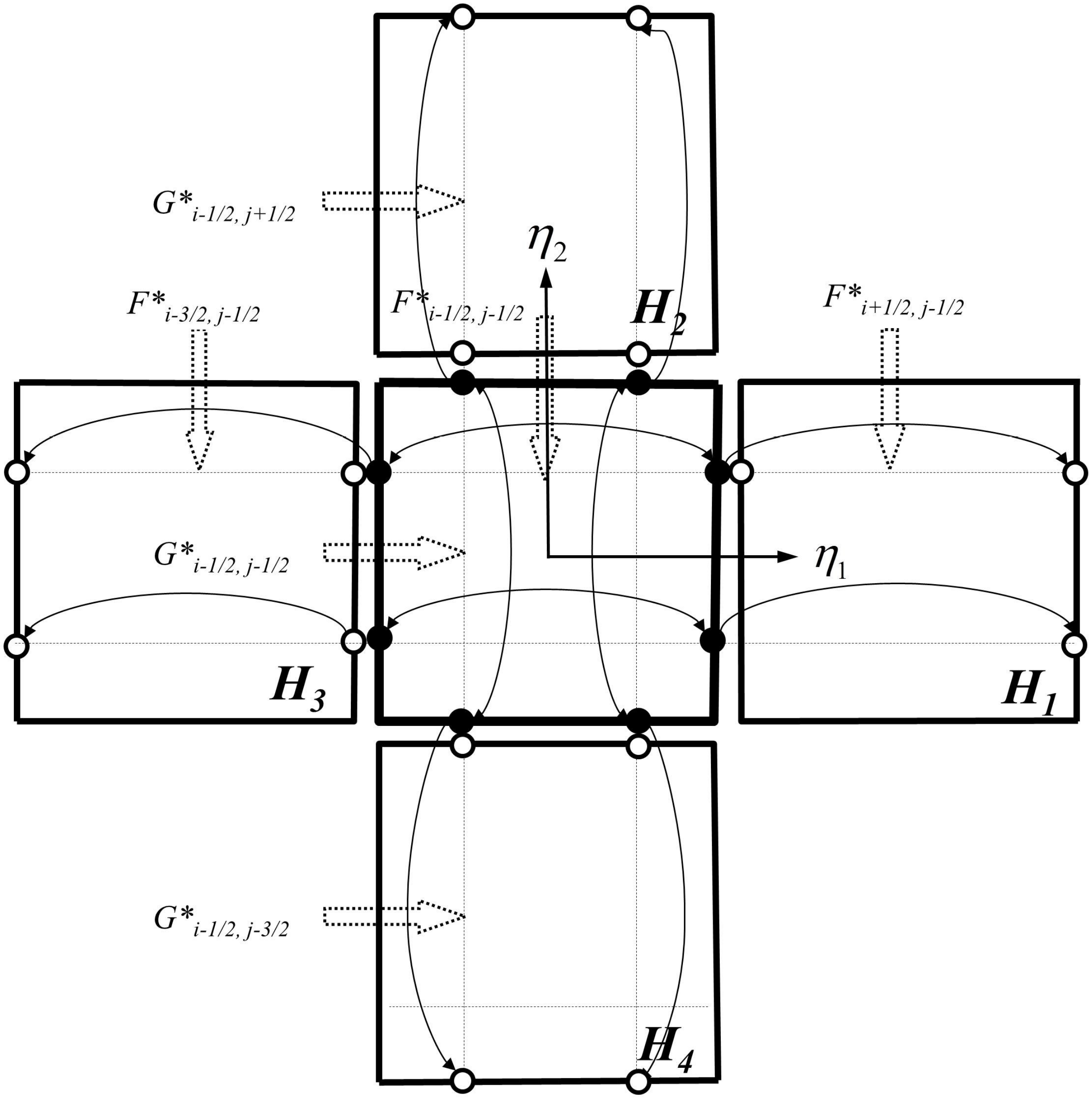

Application of the filter for triangular elements

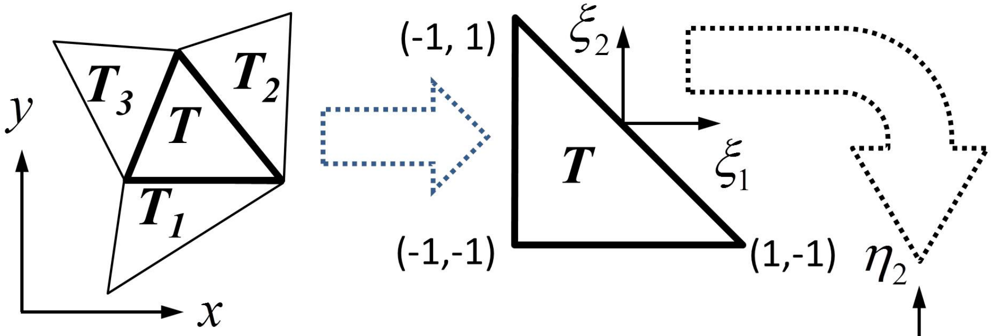

$$\eta_1 = \frac{2(1+\xi_1)}{(1-\xi_2)} - 1,$$

$$\eta_2 = \xi_2$$

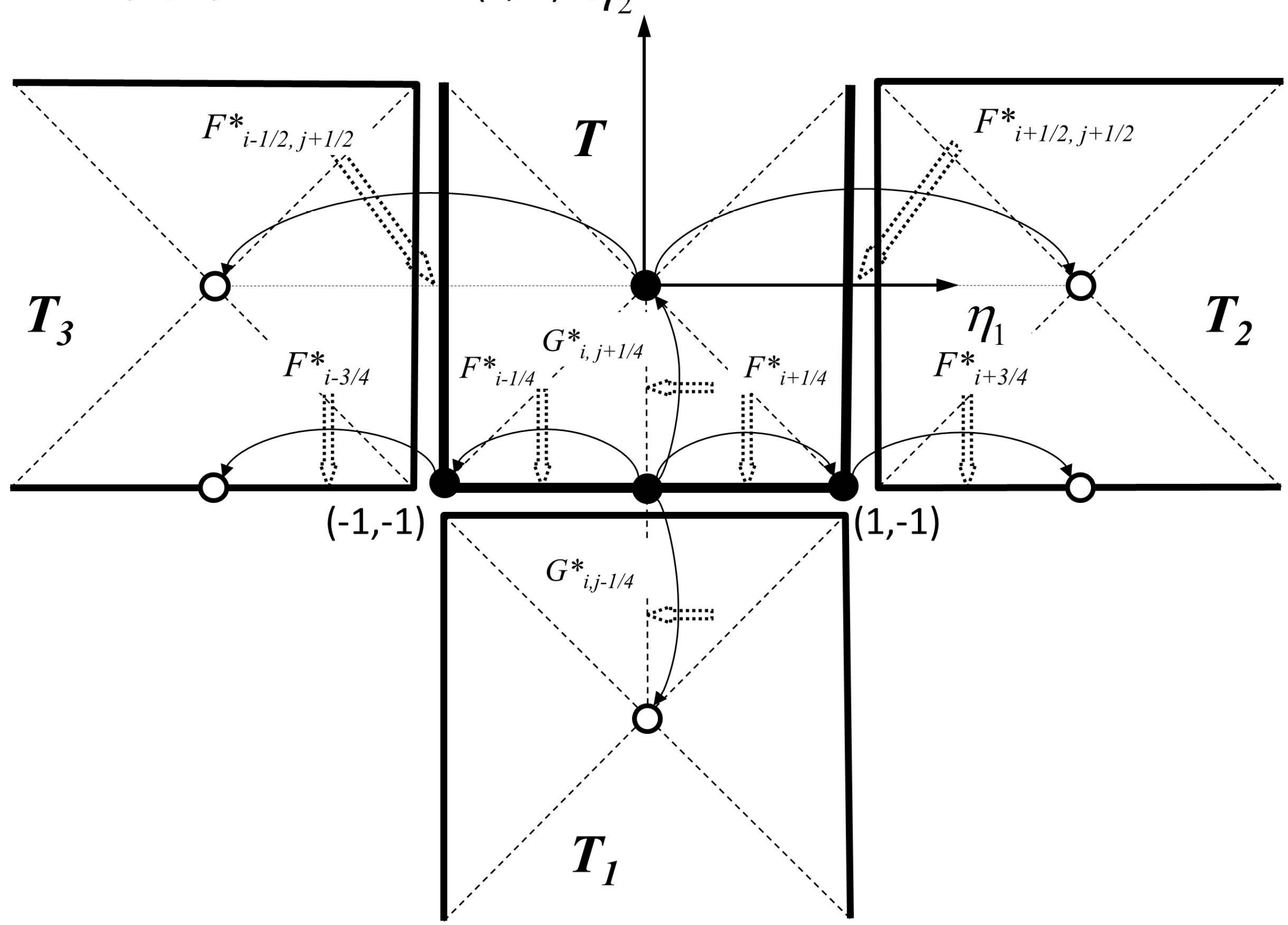

Application of the filter in 1D for P1, P2, and P3 expansions with oversampling and information only from the element

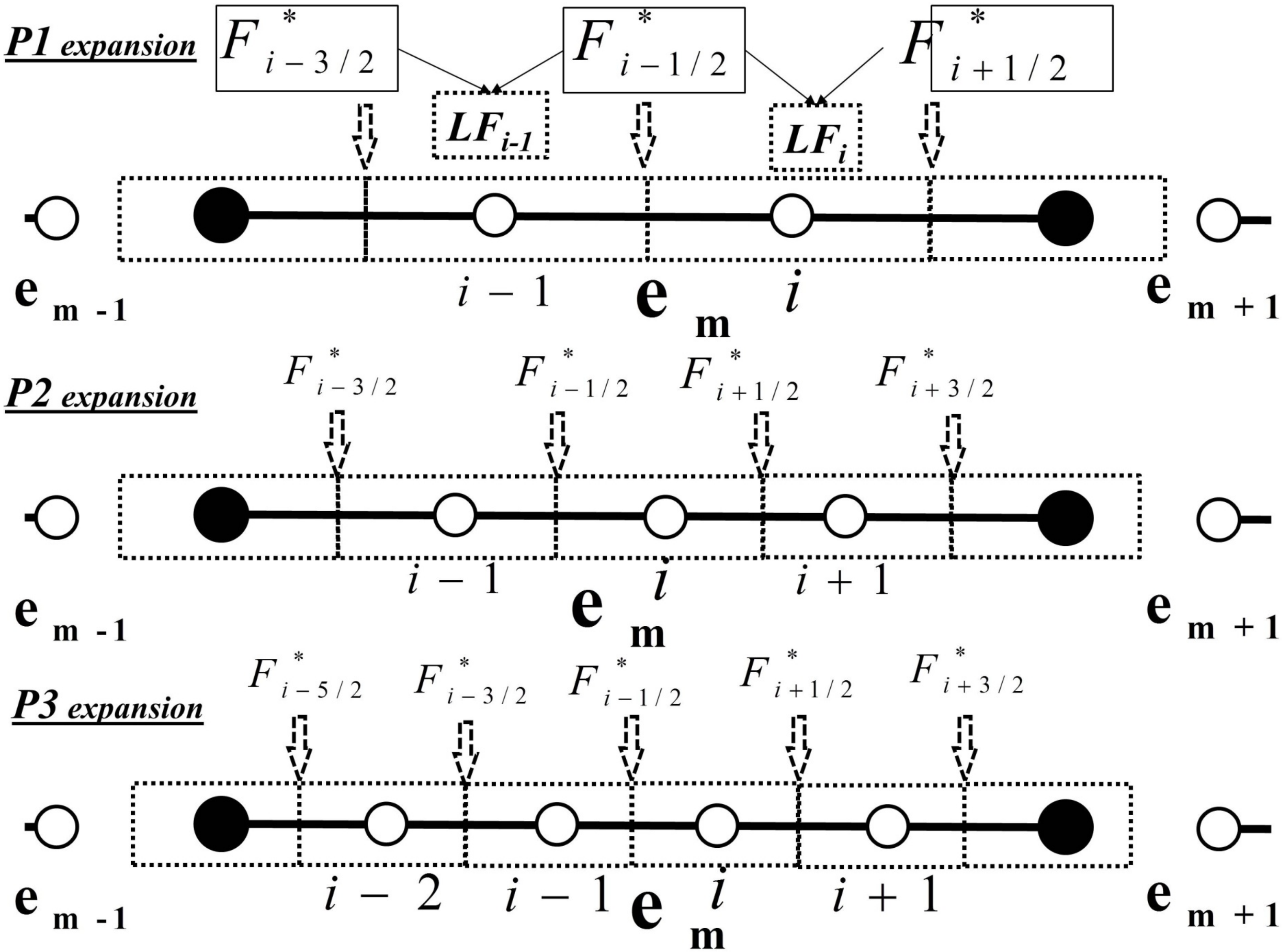

Higher order reconstruction is needed to avoid oversampling

- Use the hybridazable DG and reconstruct the numerical solution to one order higher (p to p+1) for the filter construction

- Use the recovered function (van Leer) to construct the filter operator

- Use higher order reconstruction within the element by projecting the recovered function to construct the filter operator

Application of the filter for the Sod's shock tube problem using information from neighboring elements

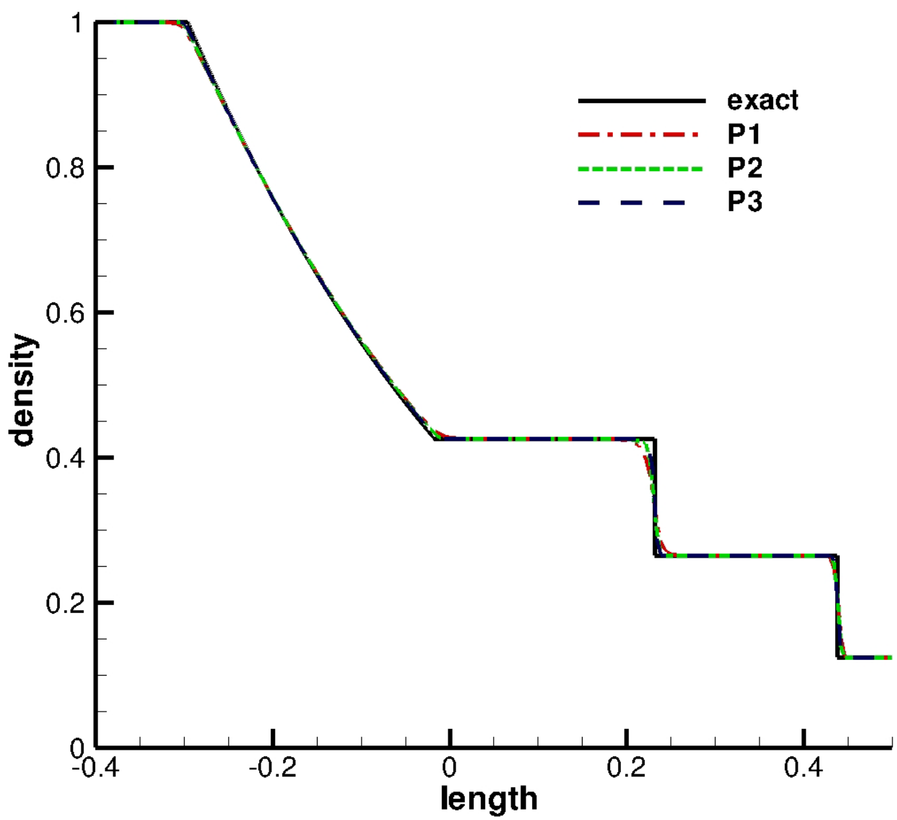

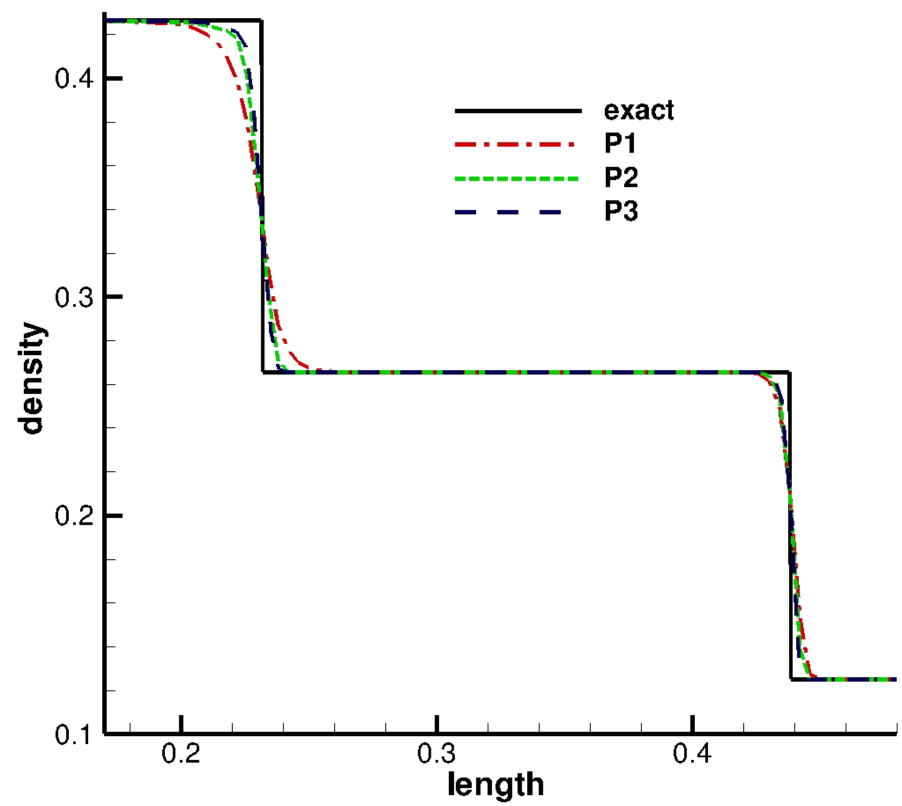

Large pressure ratio shock tube problem using information from neighboring elements

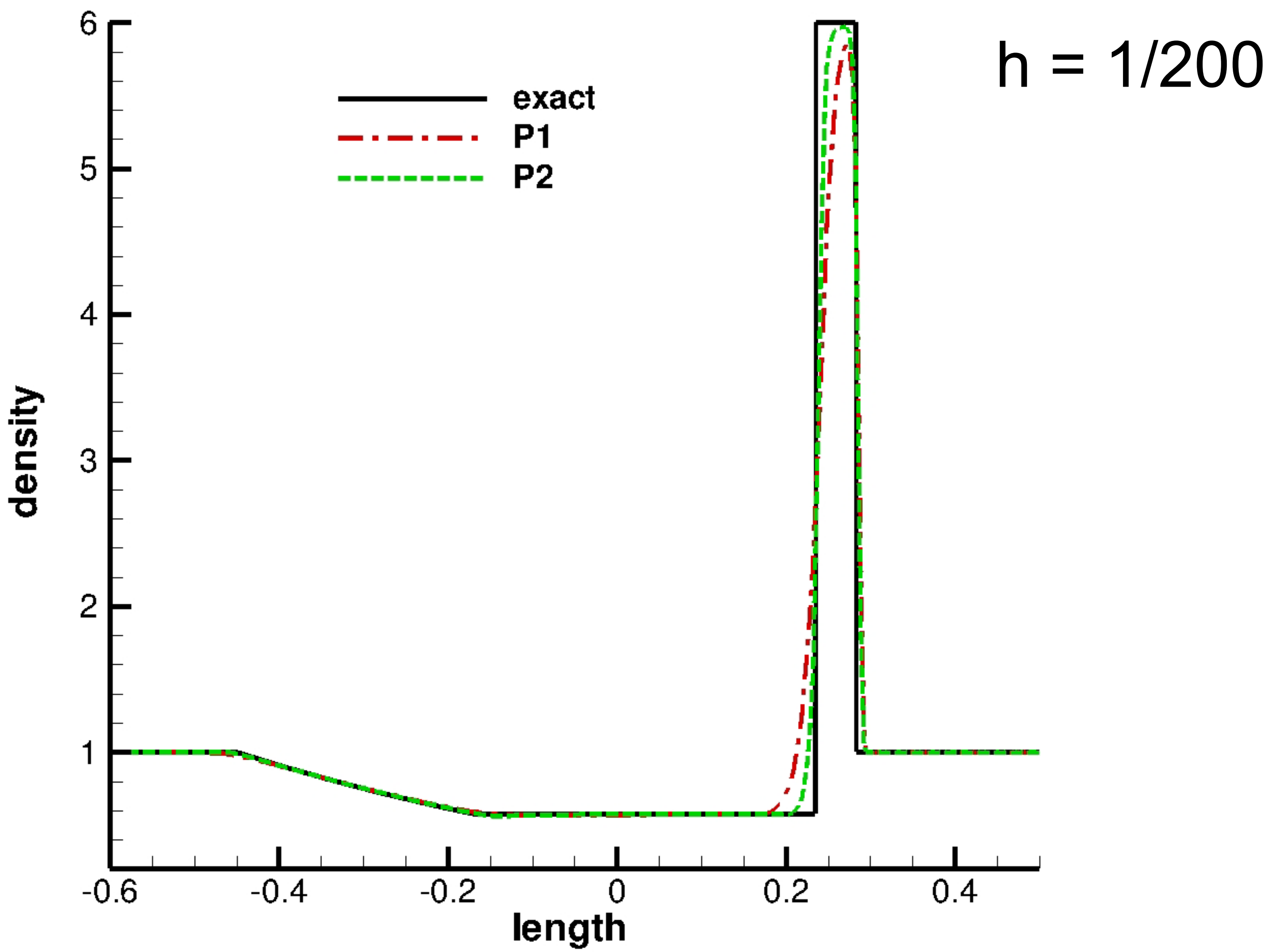

Large pressure ratio shock tube problem using information from the element

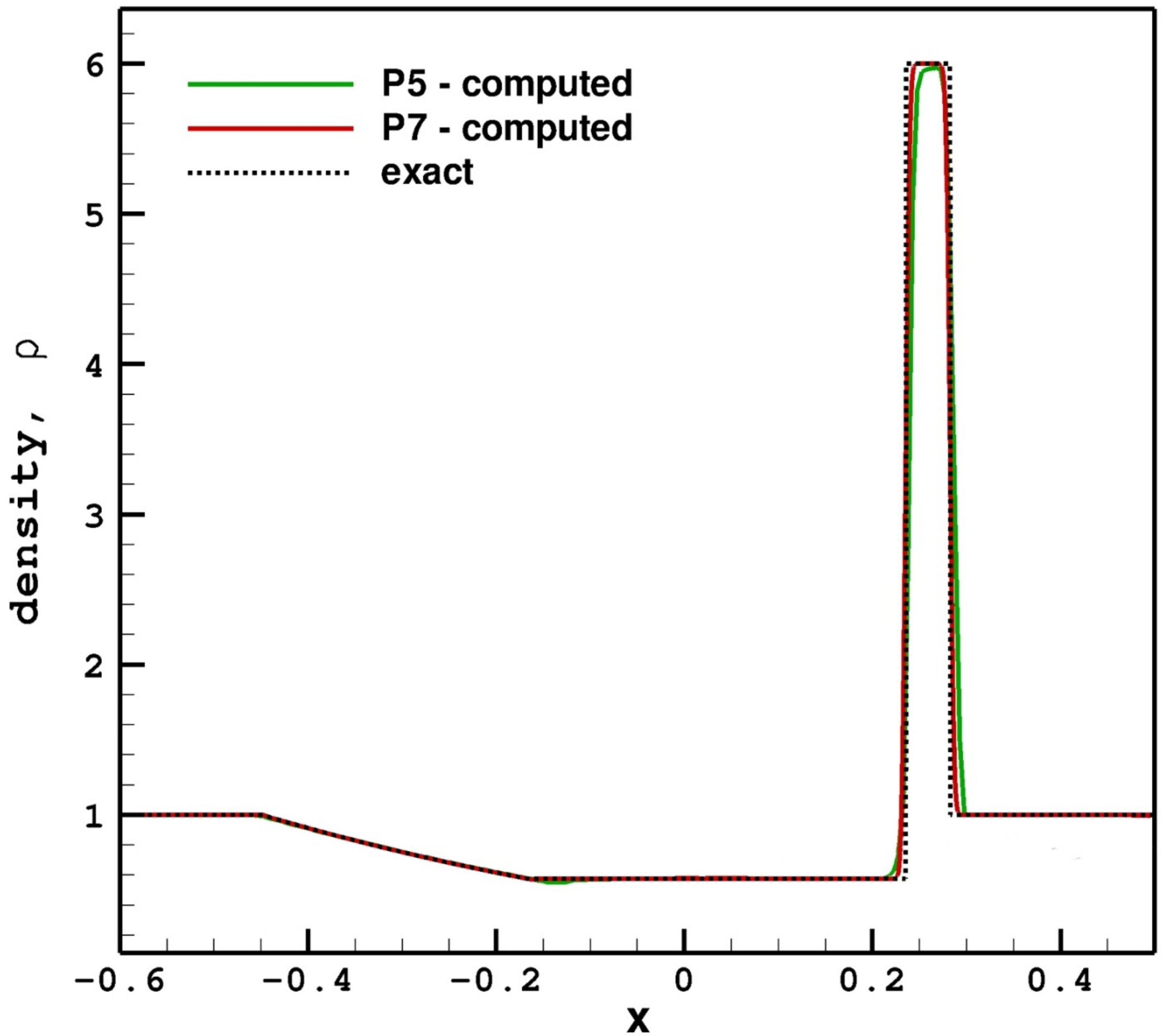

h = 1 / 40

Application of the filter for the Sod's shock tube problem sub-cell discontinuity capturing filter in the element

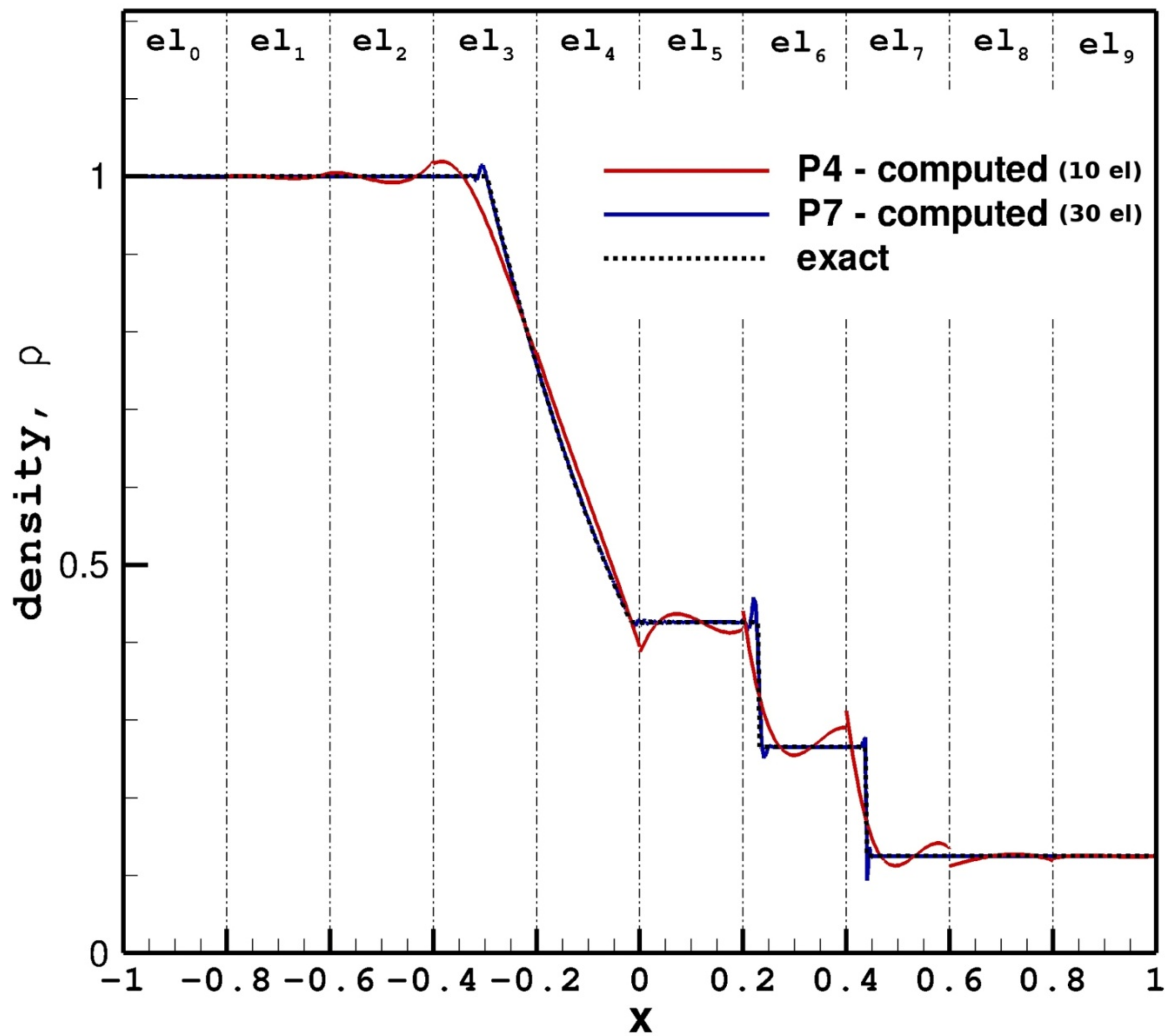

P4 h = 1/5

P7 h = 1/15

Filter operator projection with P4, h = 1/5 and in the cell discontinuity capturing

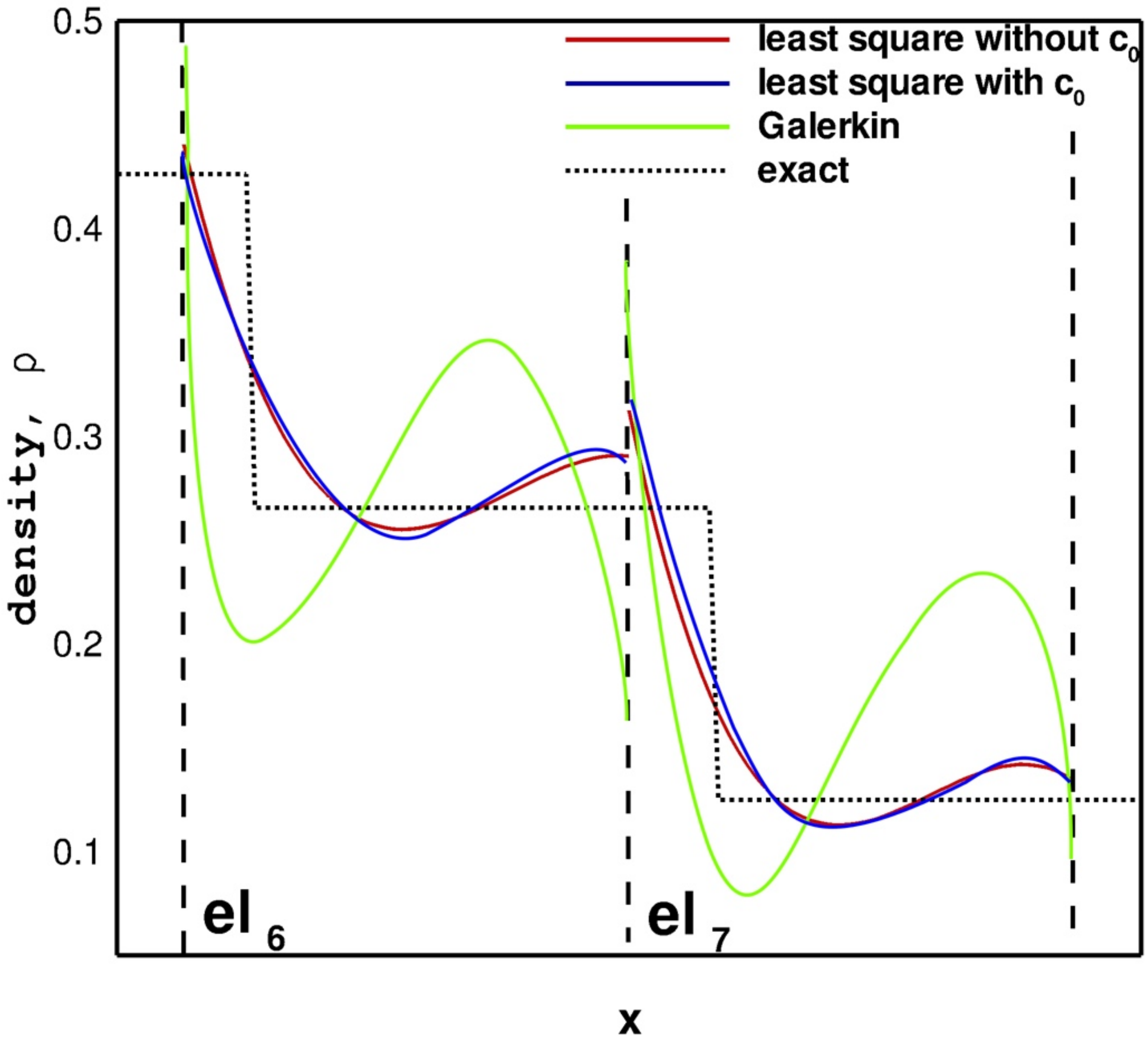

- The Galerkin projection appears more oscillatory and affects the solution average (c_0)
- Least square projection is less oscillatory and it does not require to modify the computed solution average in the spirit of TVB limiters

Convergence rate for the Sod's shock tube problem filter operator from the element

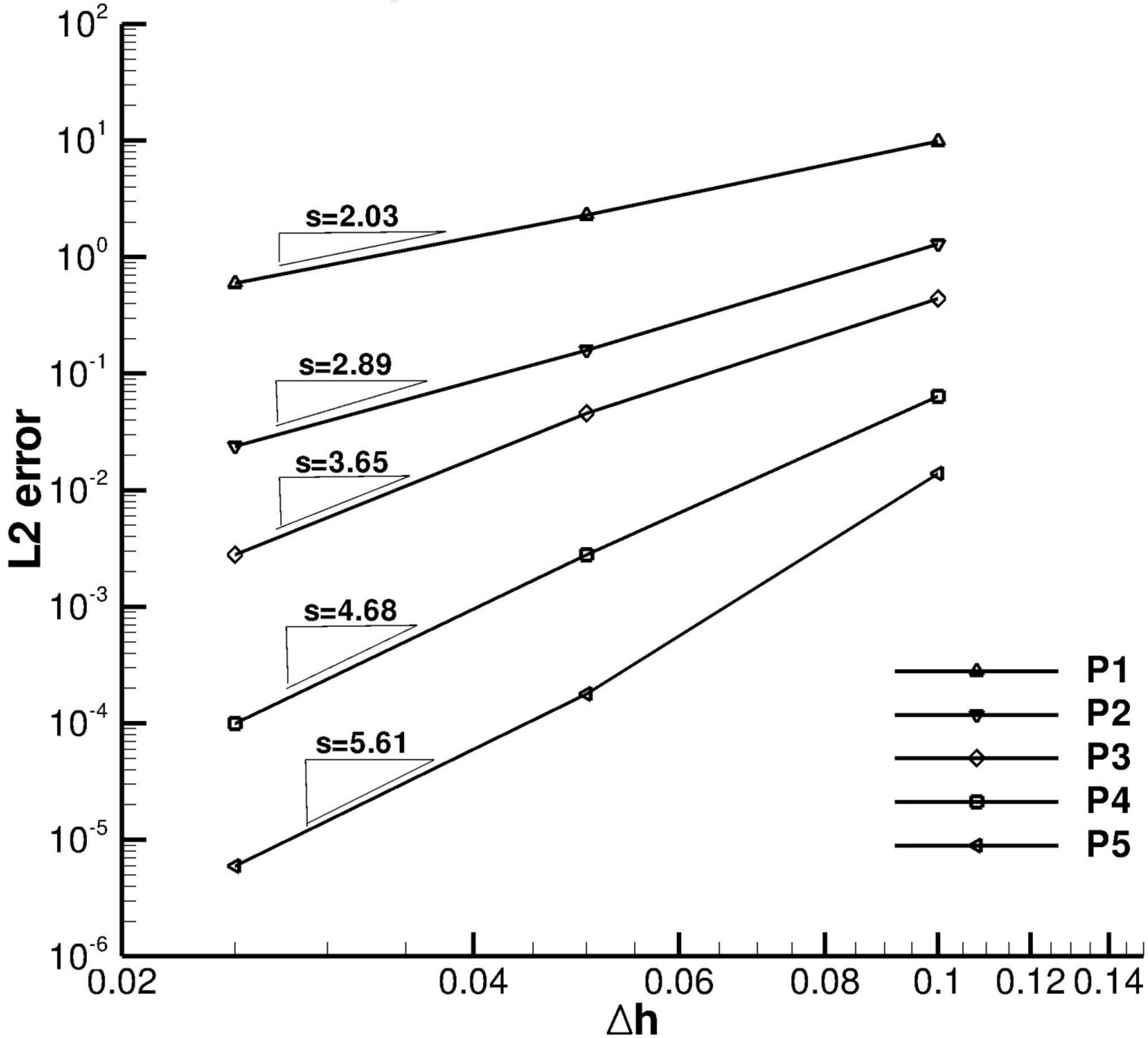

Shu and Osher density perturbation shock interaction using information from neighboring elements

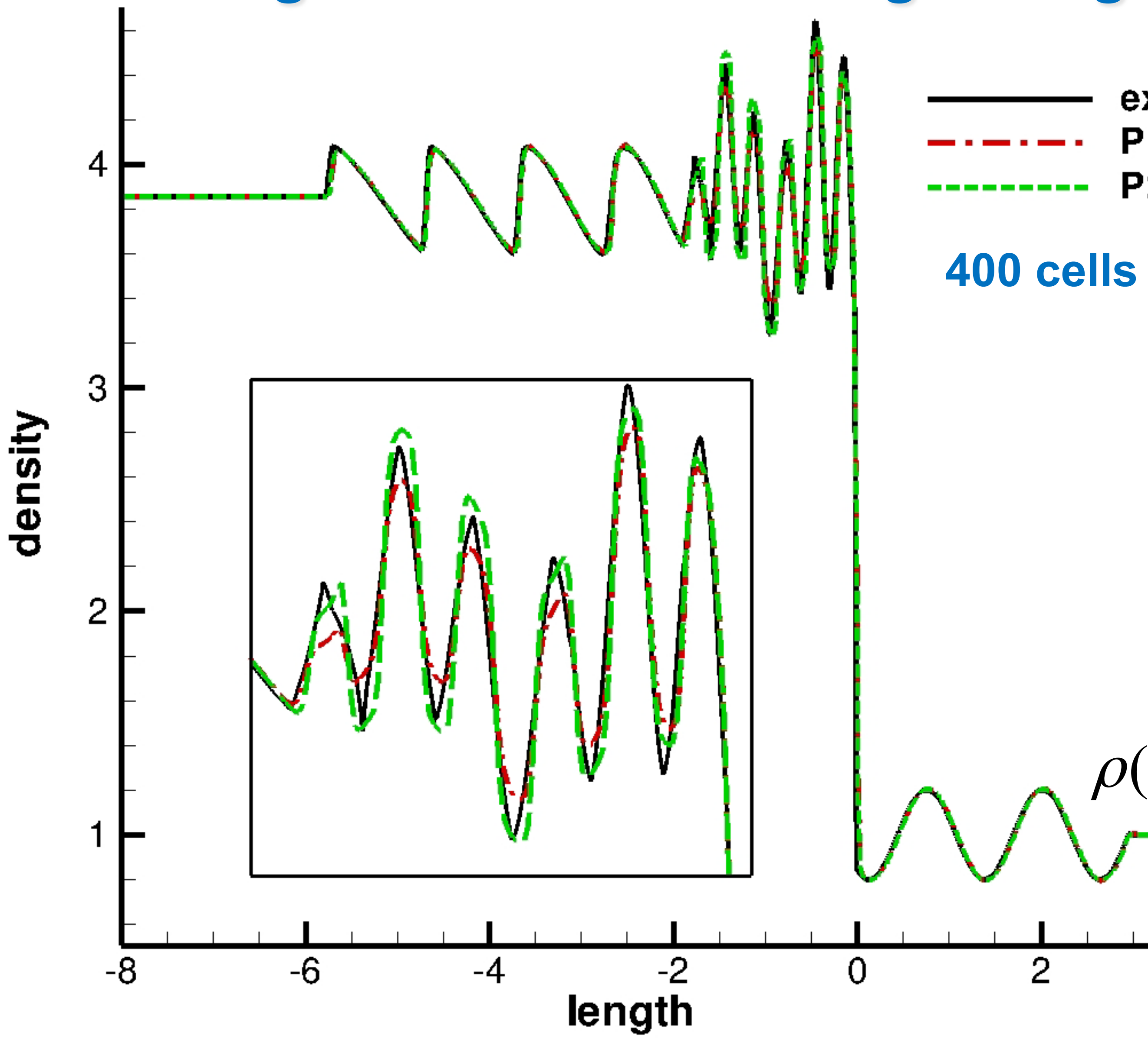

$$\rho(x) = 1 + 0.2\sin(5x)$$

Shu and Osher density perturbation shock interaction using information from the element

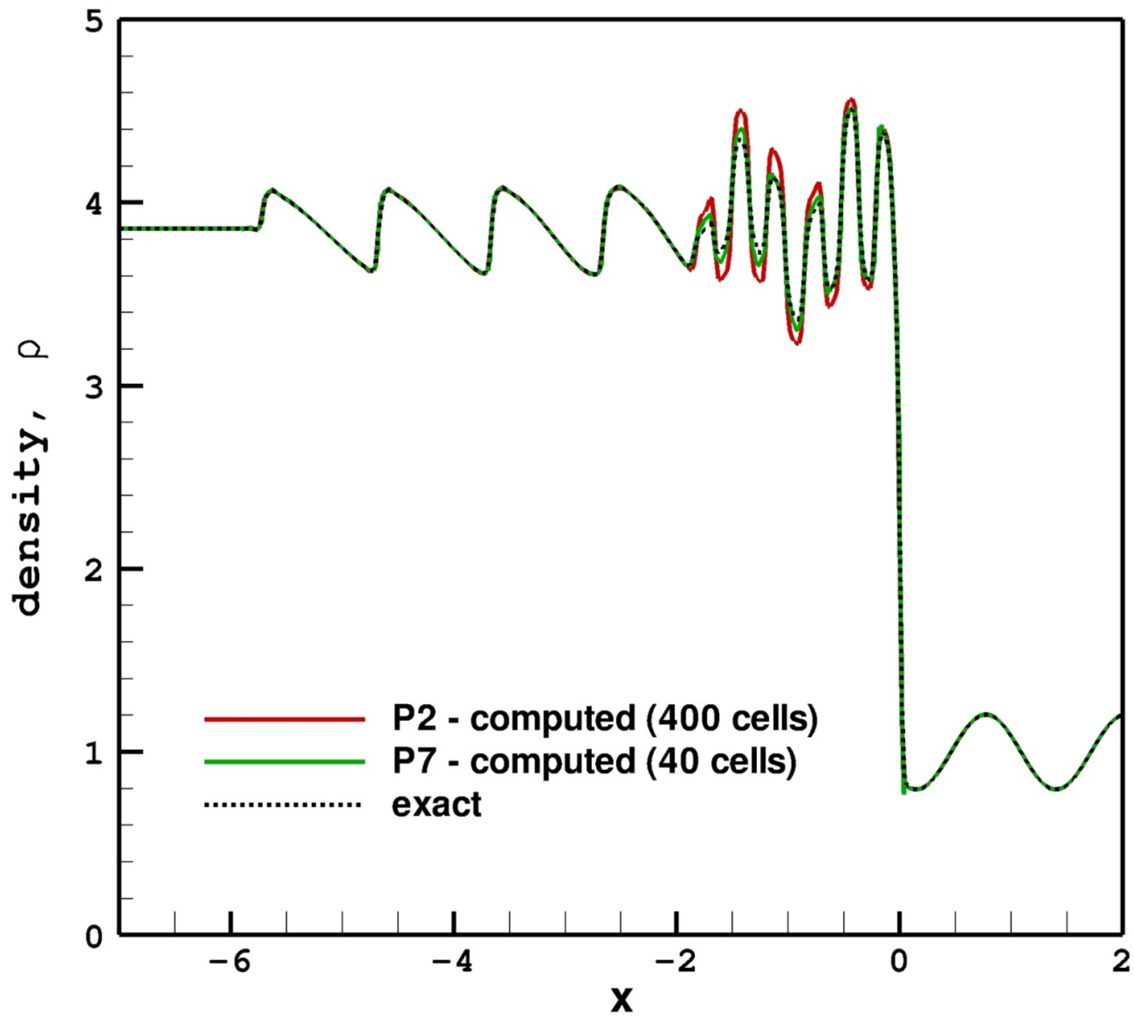

NACA-0012 airfoil at M = 0.8, $\alpha = 1.25^o$

P4 numerical solution P2 surface elements

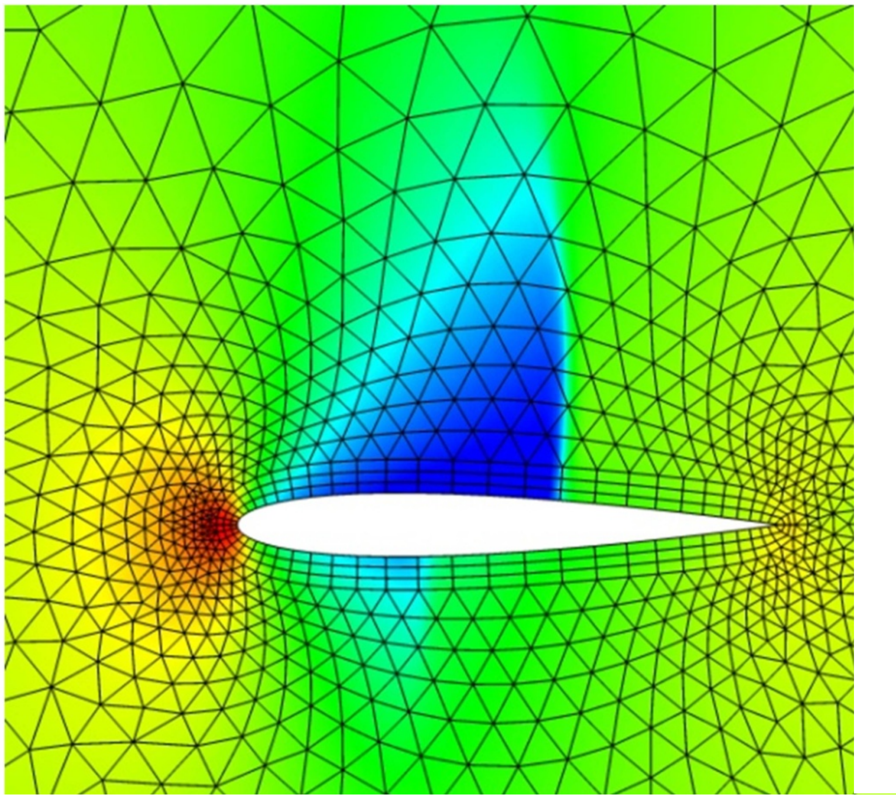

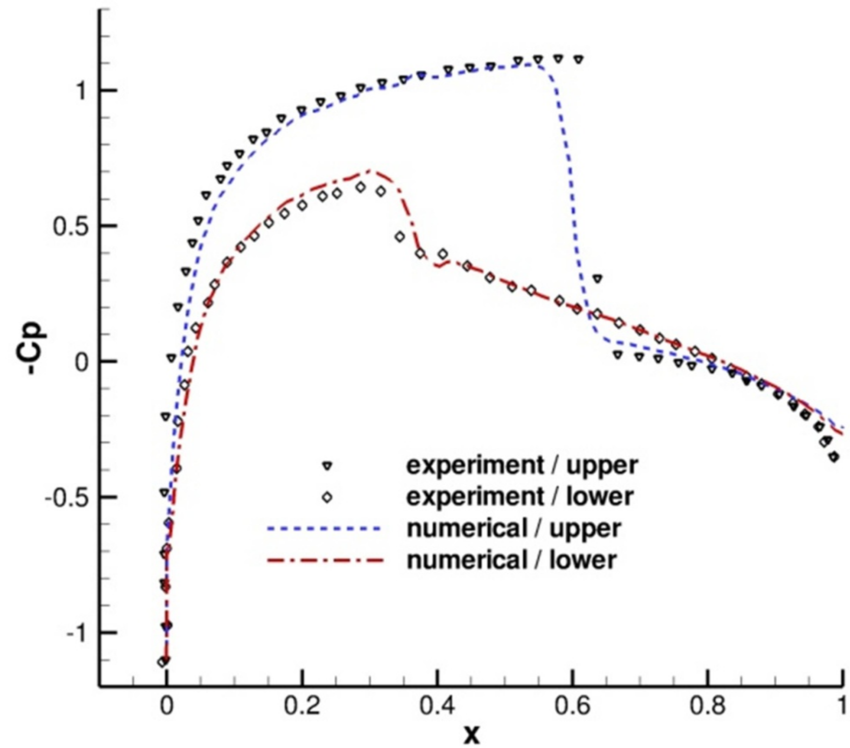

M=3, β=30 oblique shock reflection

Convergence to the design order of accuracy has been achieved

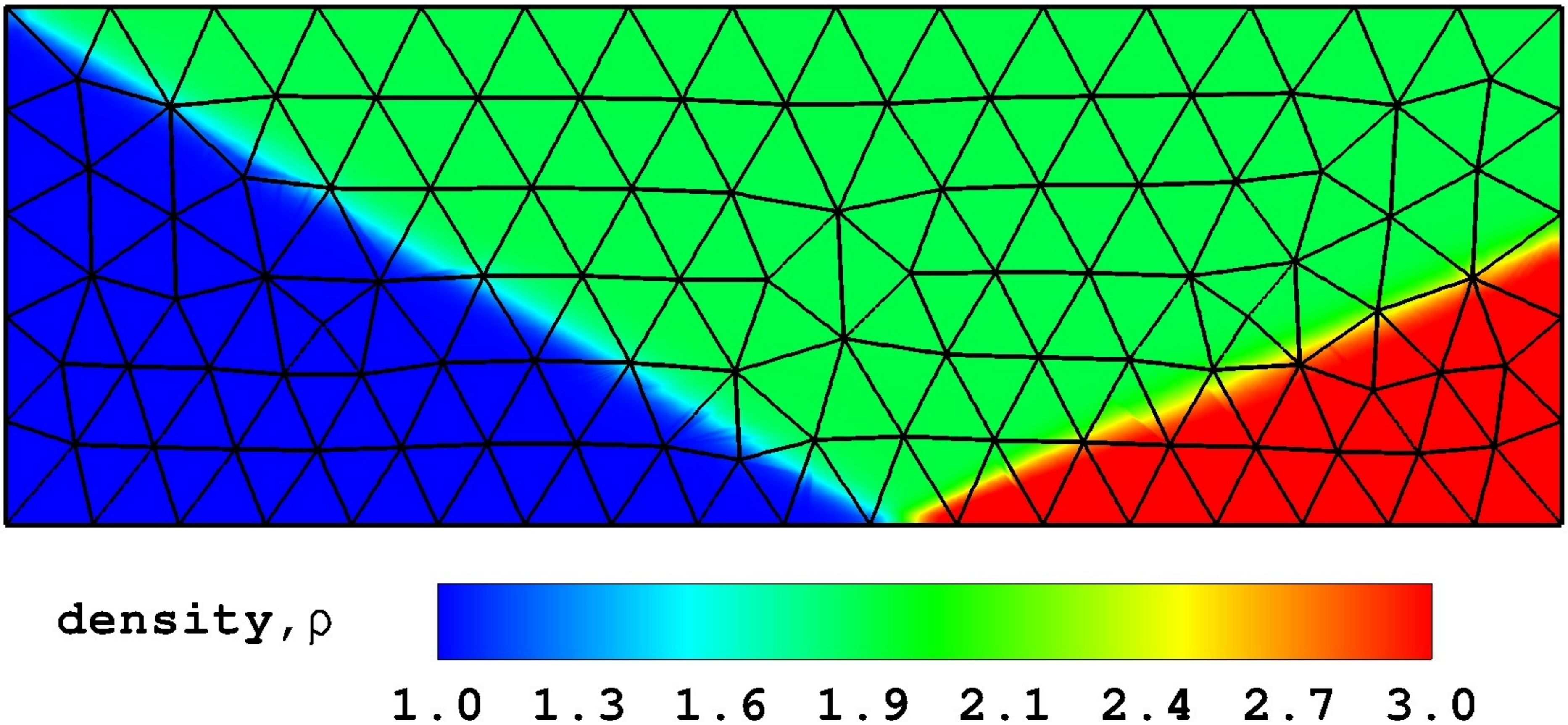

Flow at M = 3 in a tunnel with a step

P1
Filtered
h = 1/80

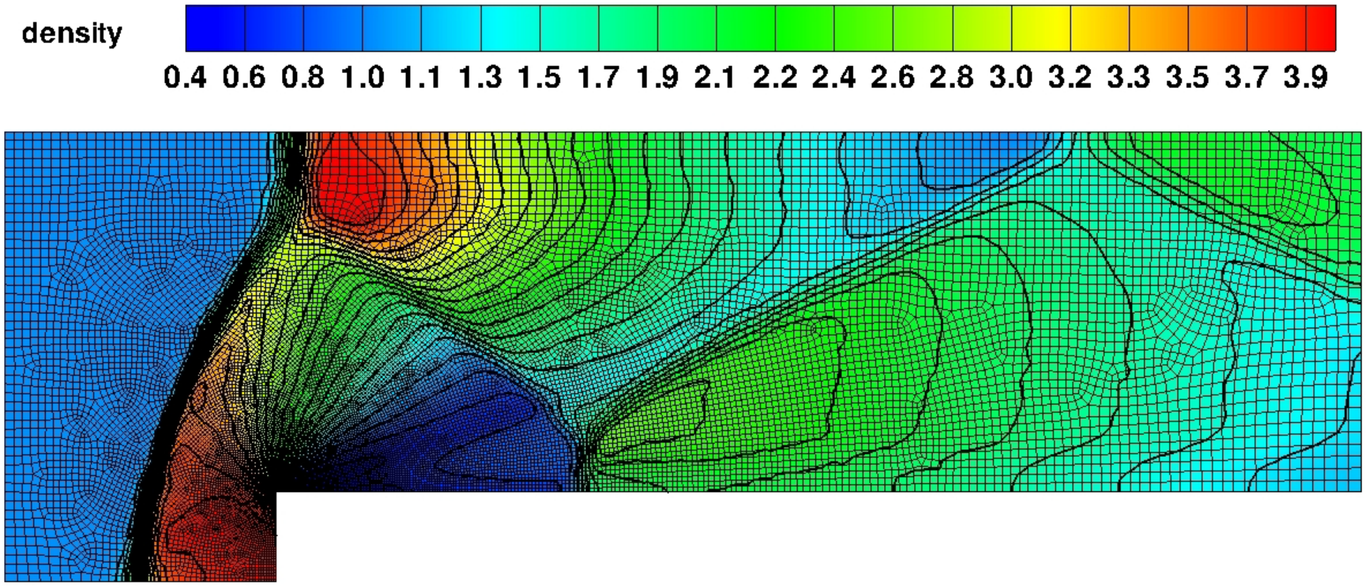

P1
TVB limiter
H = 1/120

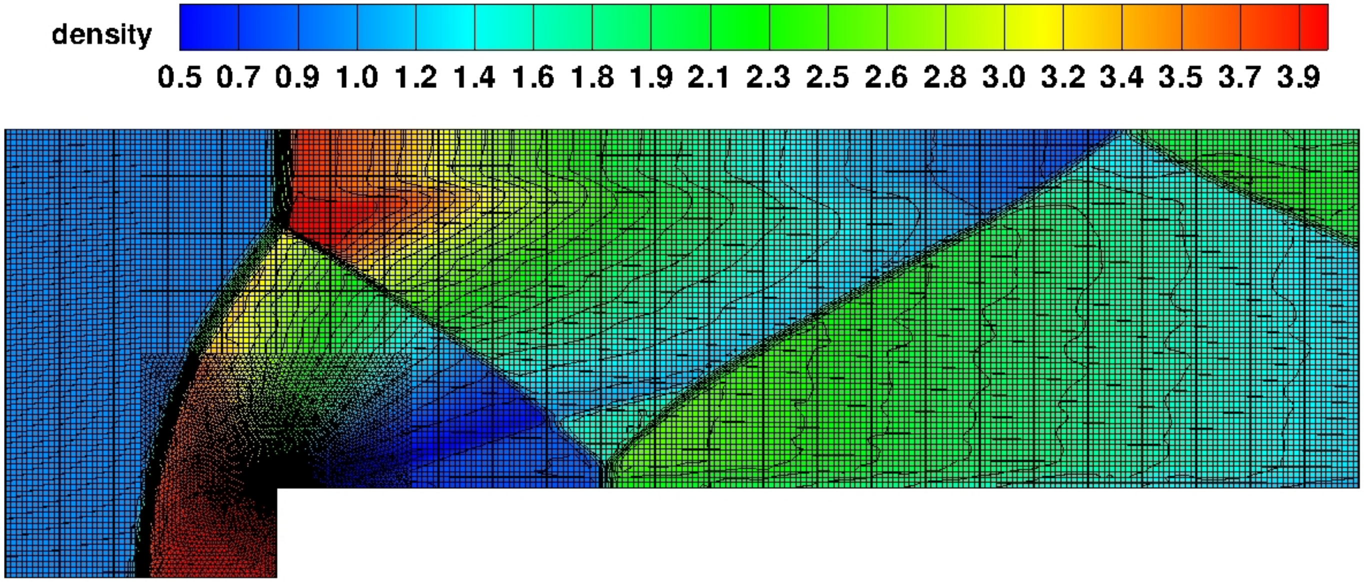

Flow at M = 3 in a tunnel with a step

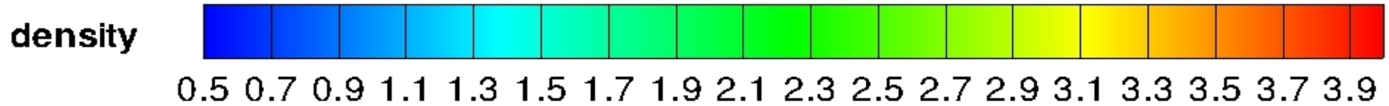

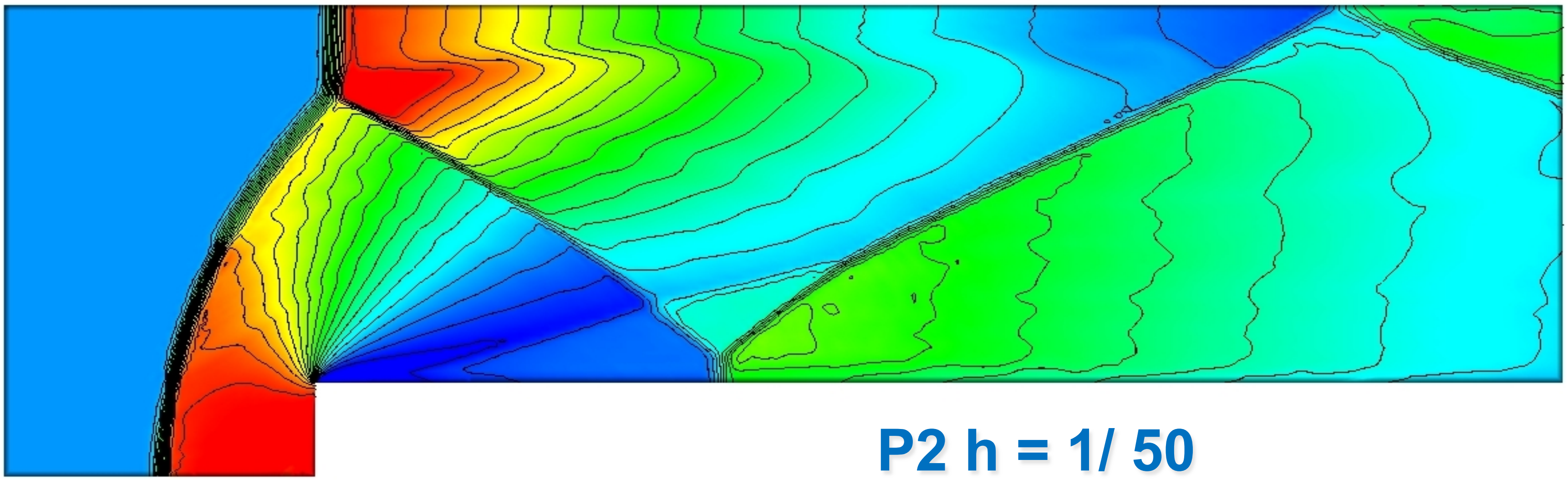

P2 h = 1/ 50

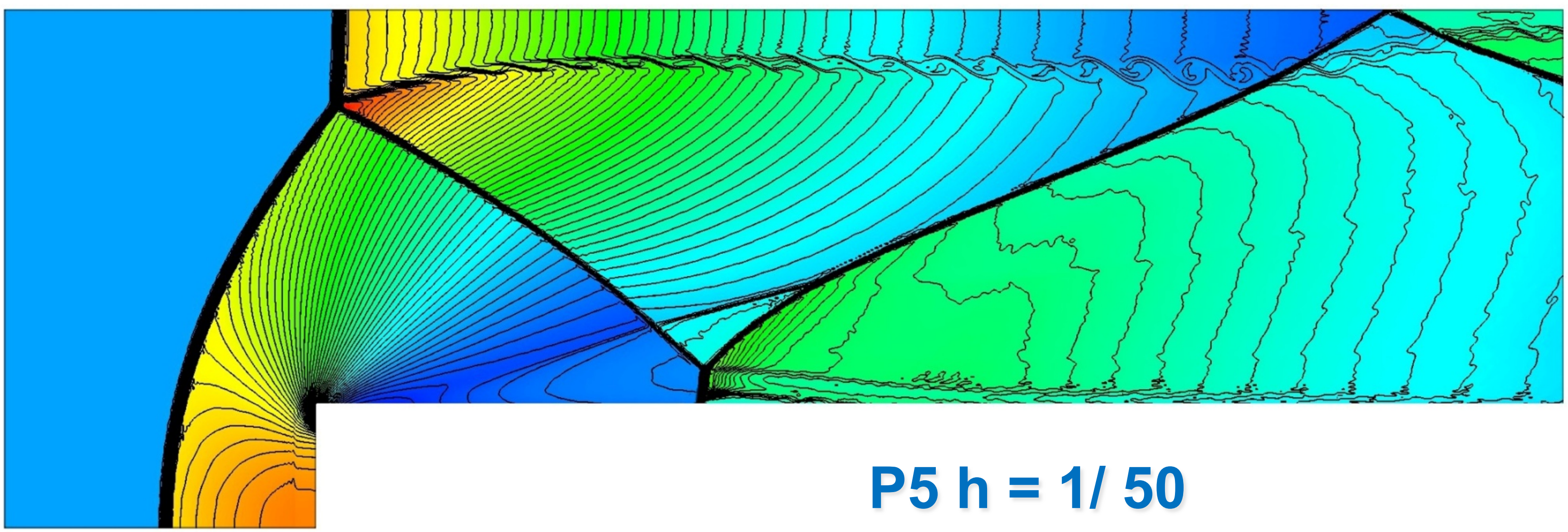

P5 h = 1/ 50

Reflection of a M=2 shock from a wavy

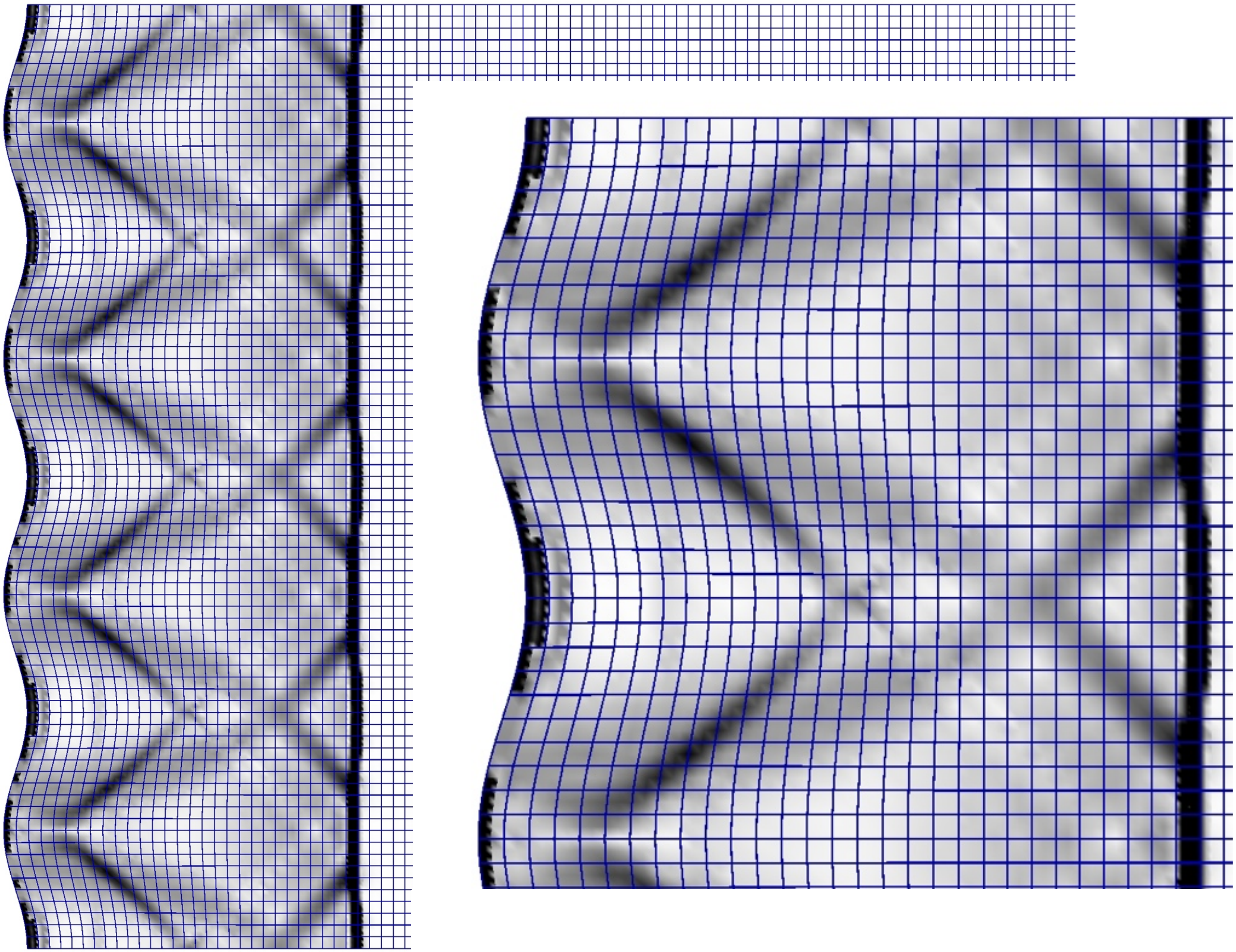

Flow at M = 3 in a tunnel with a step

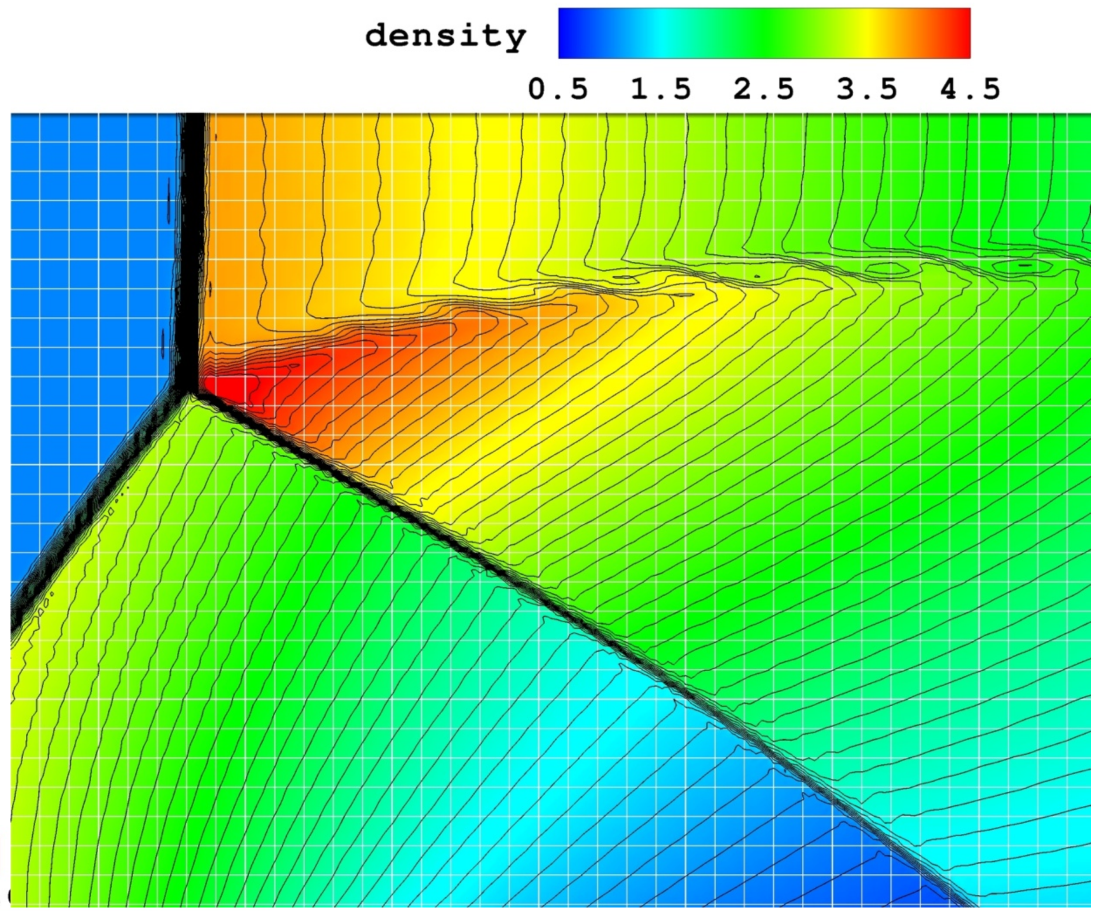

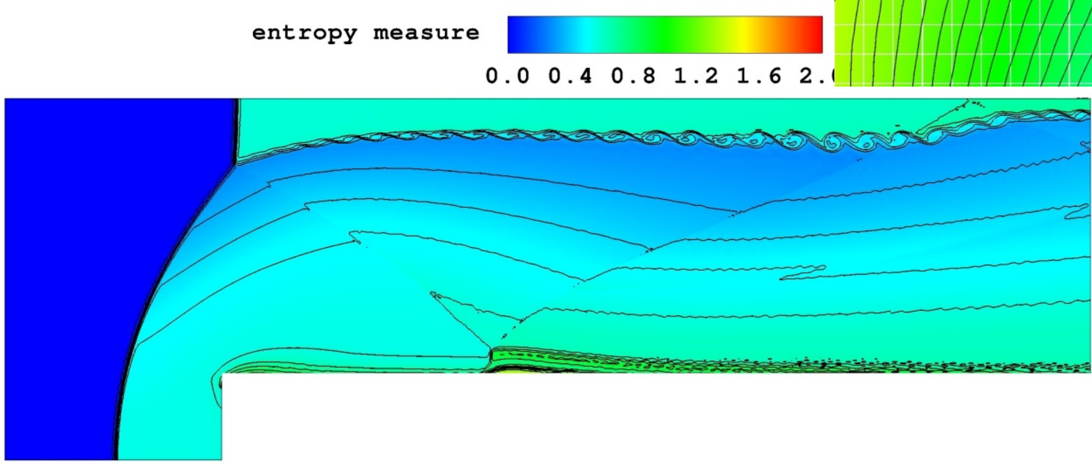

P5 h = 1/ 50

Transonic flow at M = 0.8, ONERA M6 wing, P1

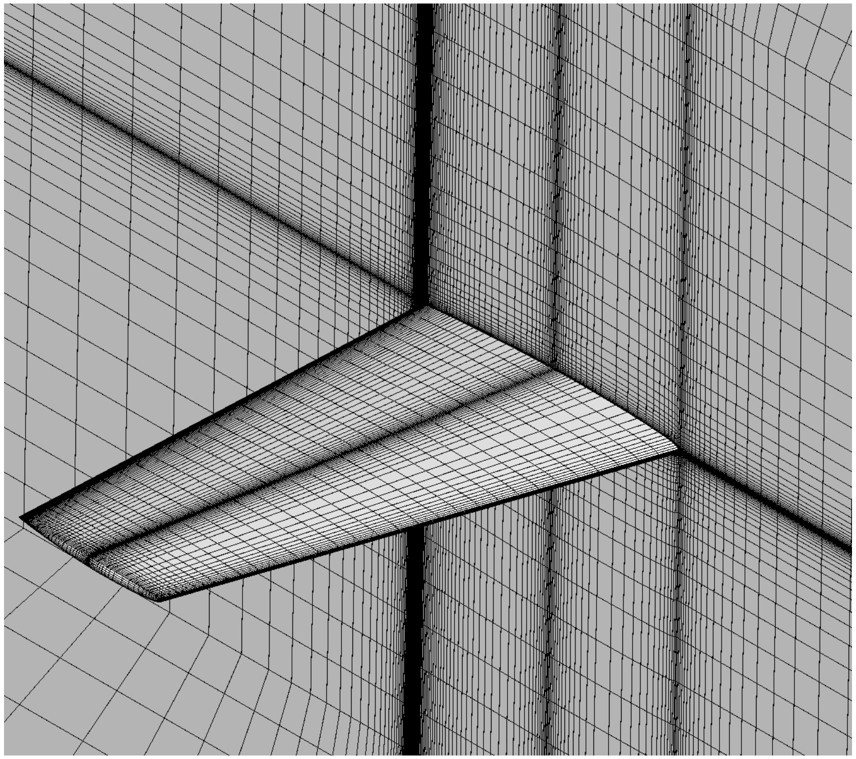

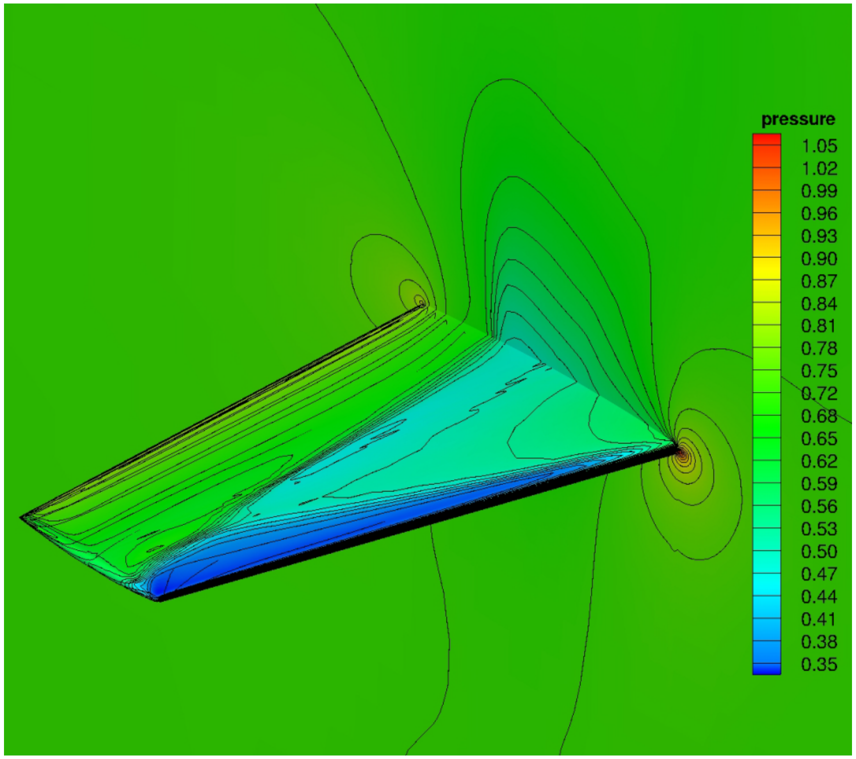

ONERA M6 wing P1 solution at M = 0.8

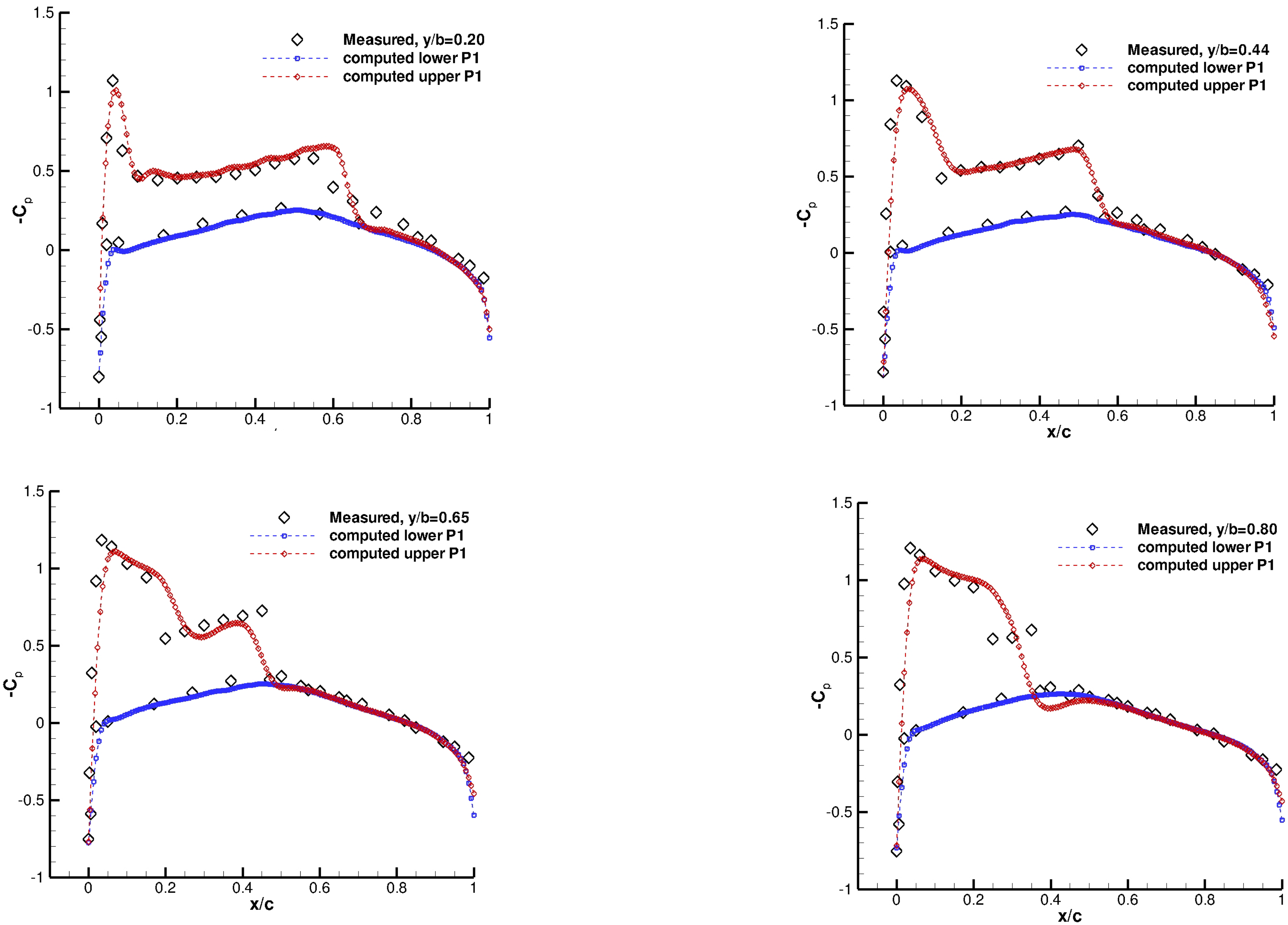

ONERA M6 wing M = 0.8, P3 sub-cell shock capturing

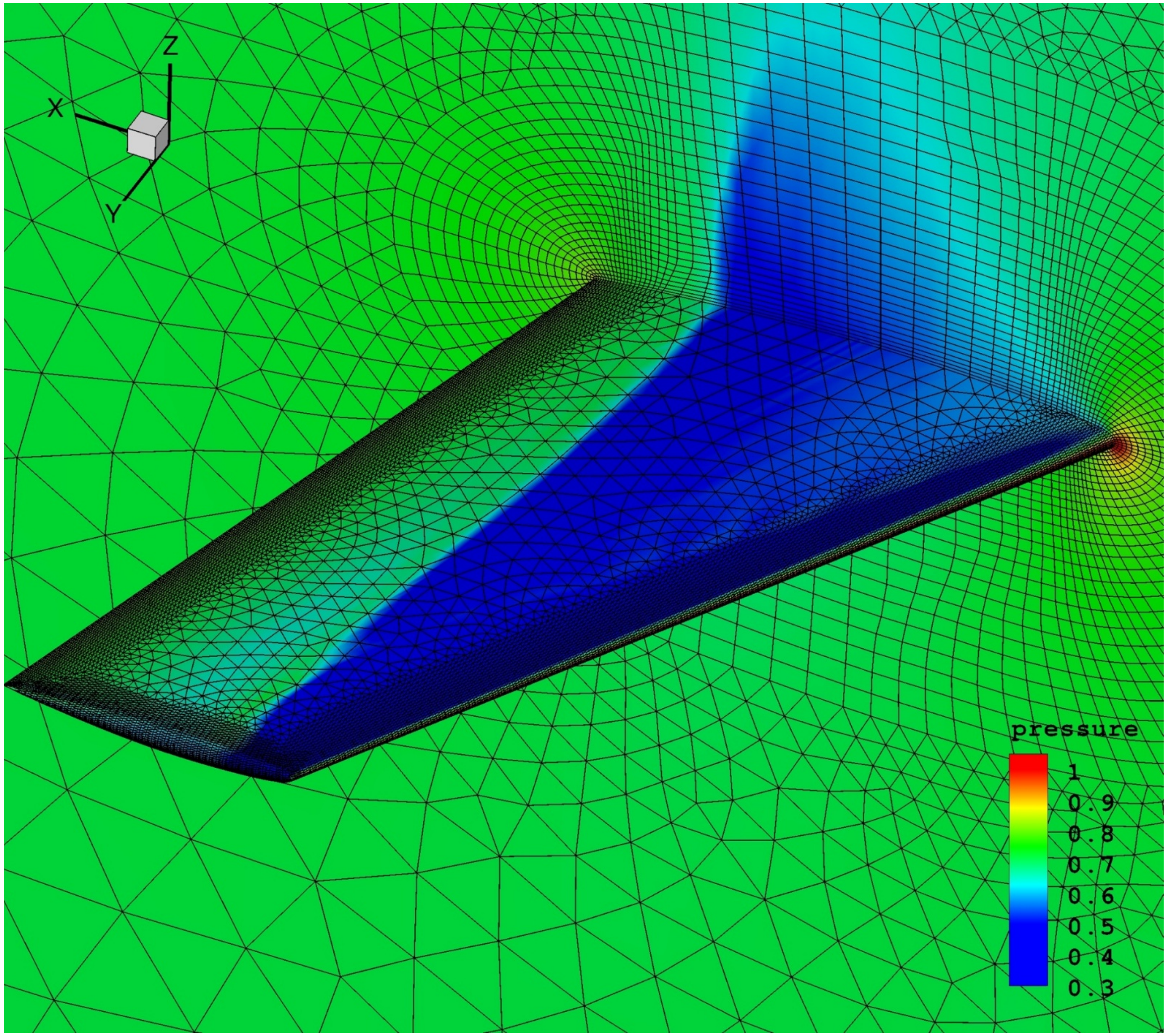

ONERA M6 wing P3 solution at M = 0.8

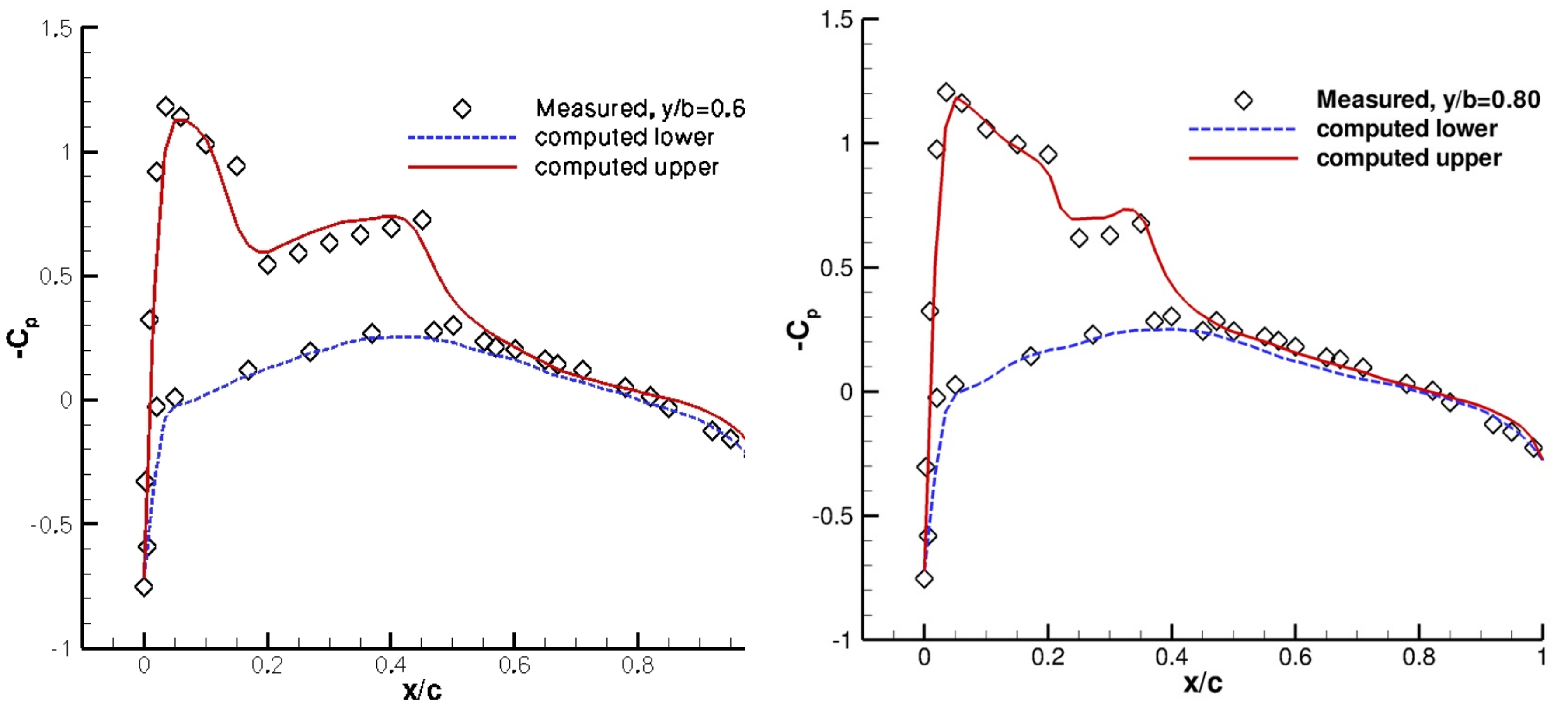

ONERA M6 wing M = 0.8, P4-P5 shock capturing

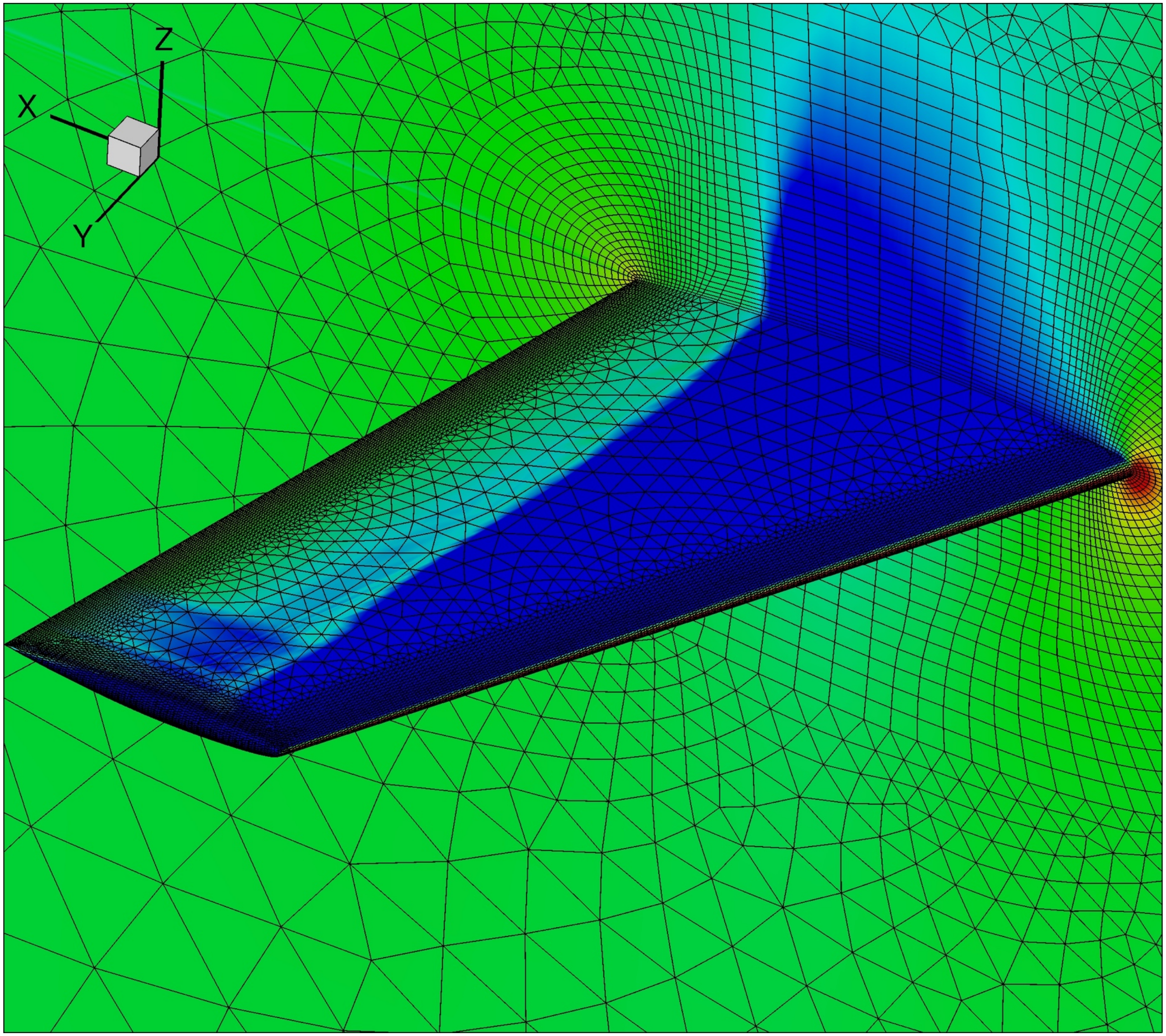

h/p adaptivity for chemically reacting flow at M = 0.8

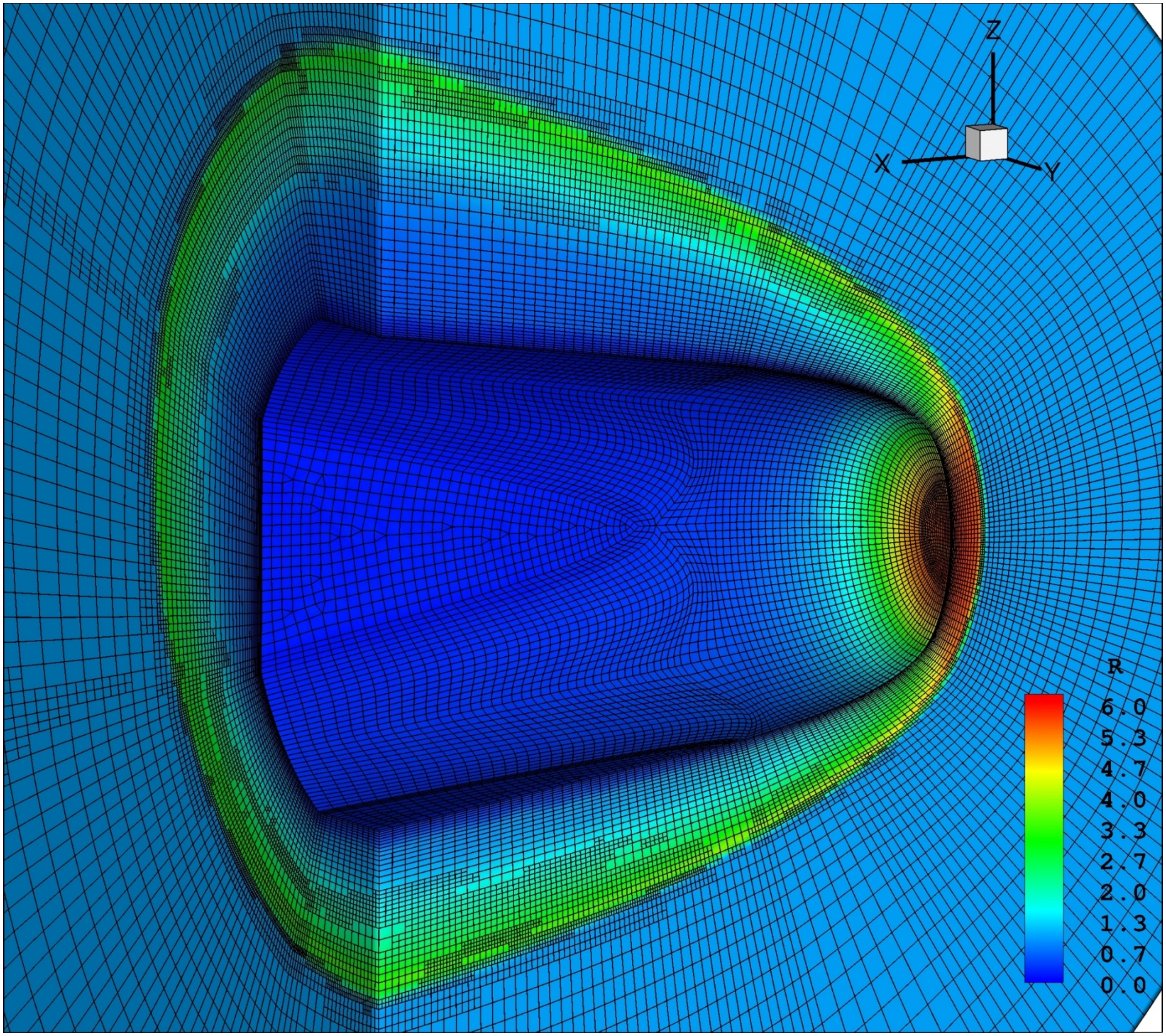

Chemically reacting flow at M = 0.8

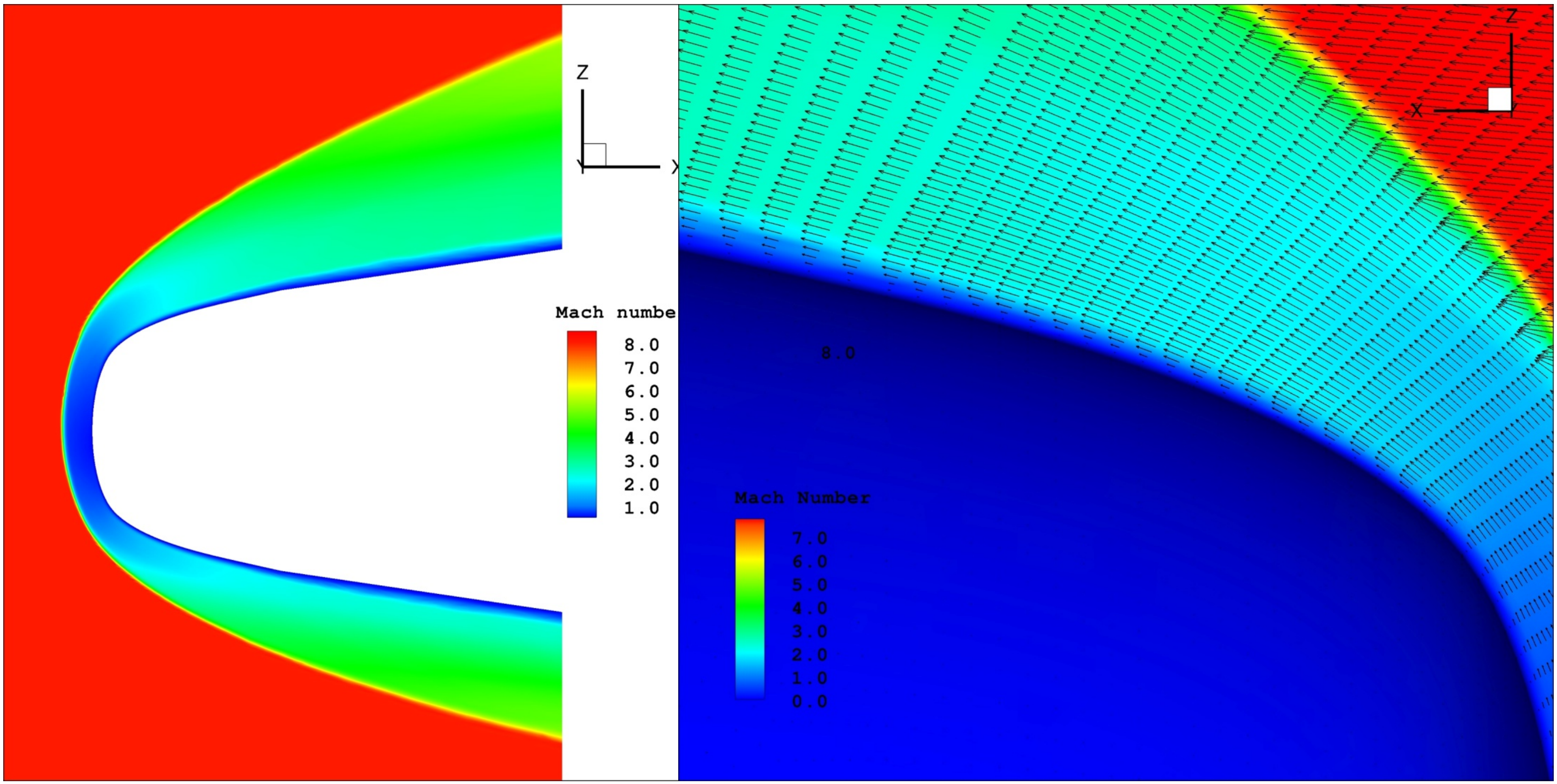

Chemically reacting flow at M = 0.8

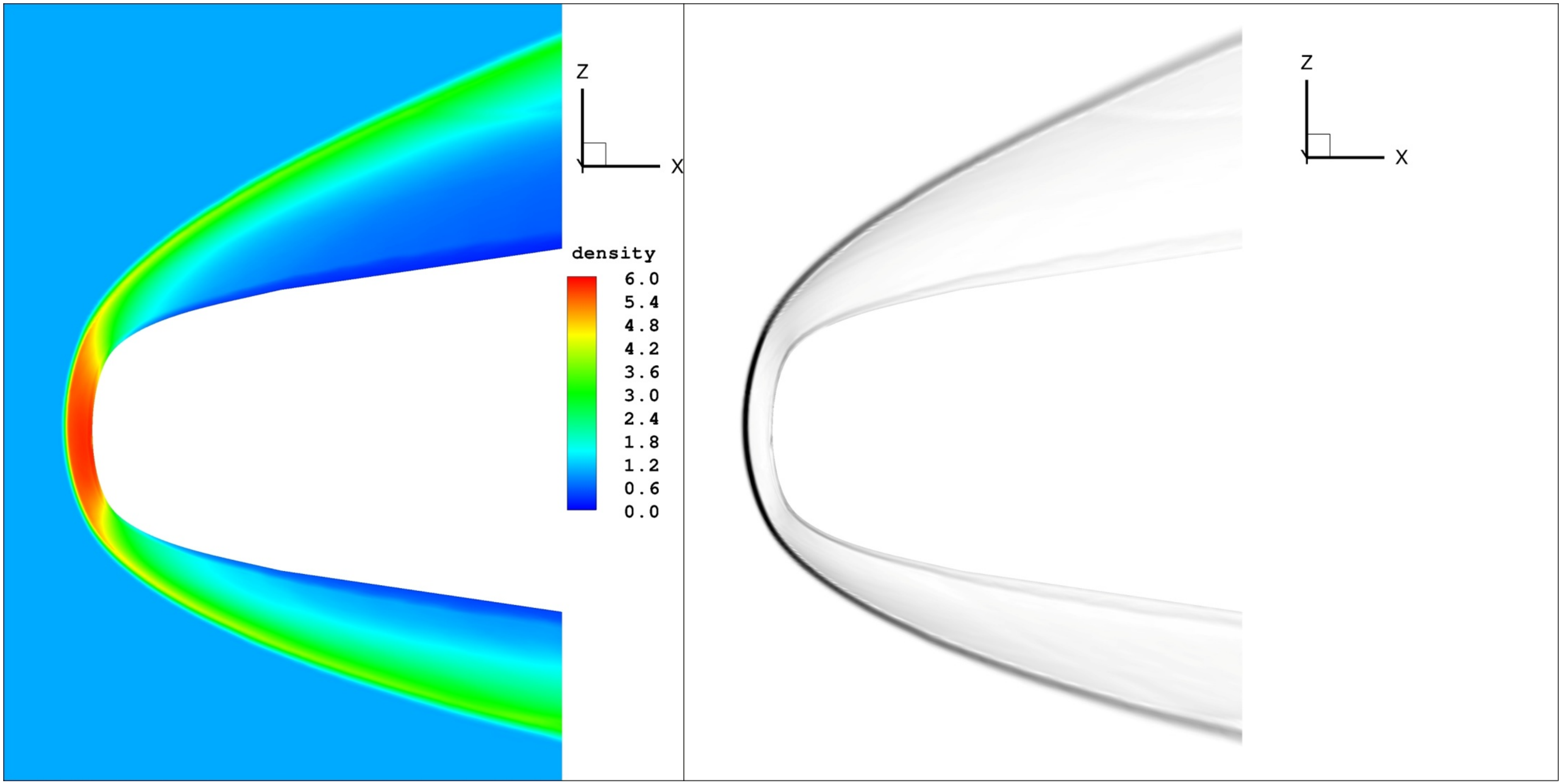

h/p adaptivity for chemically reacting flow at M = 0.8

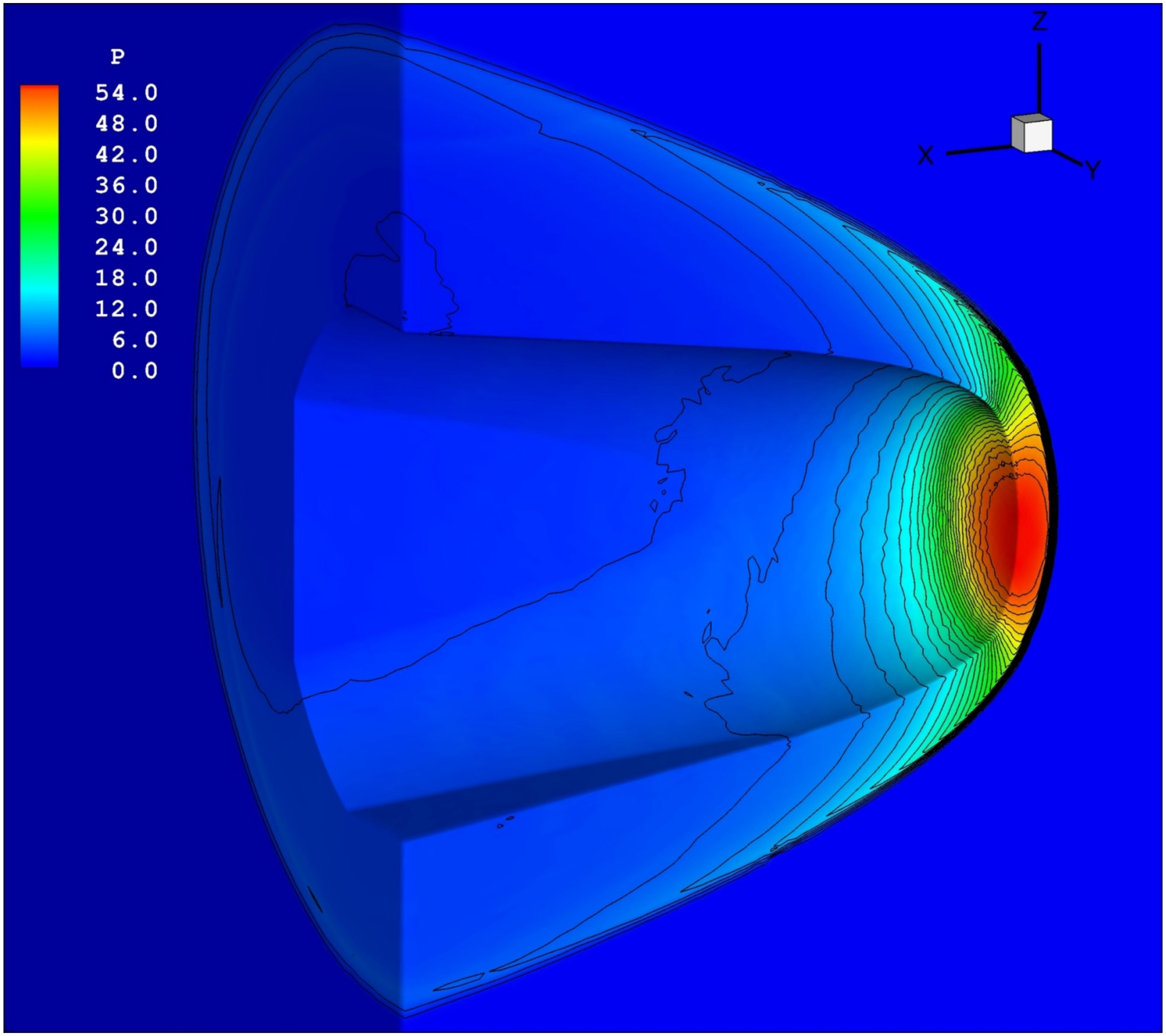

Chemically reacting flow at M = 0.8

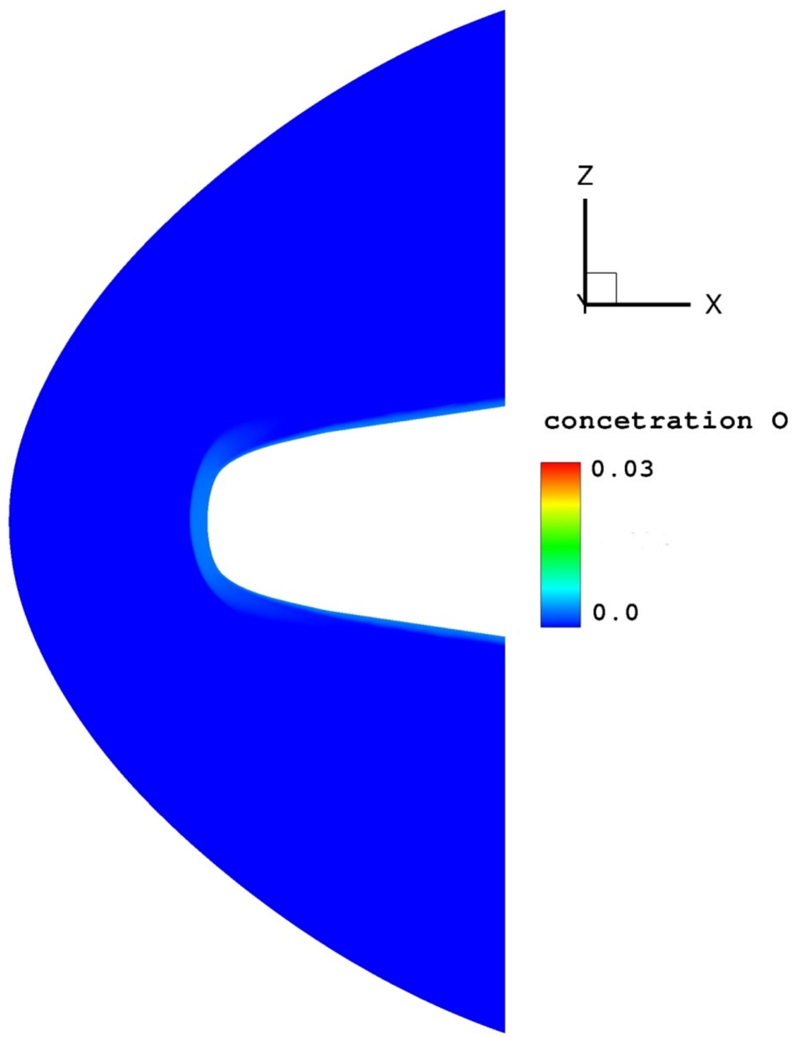

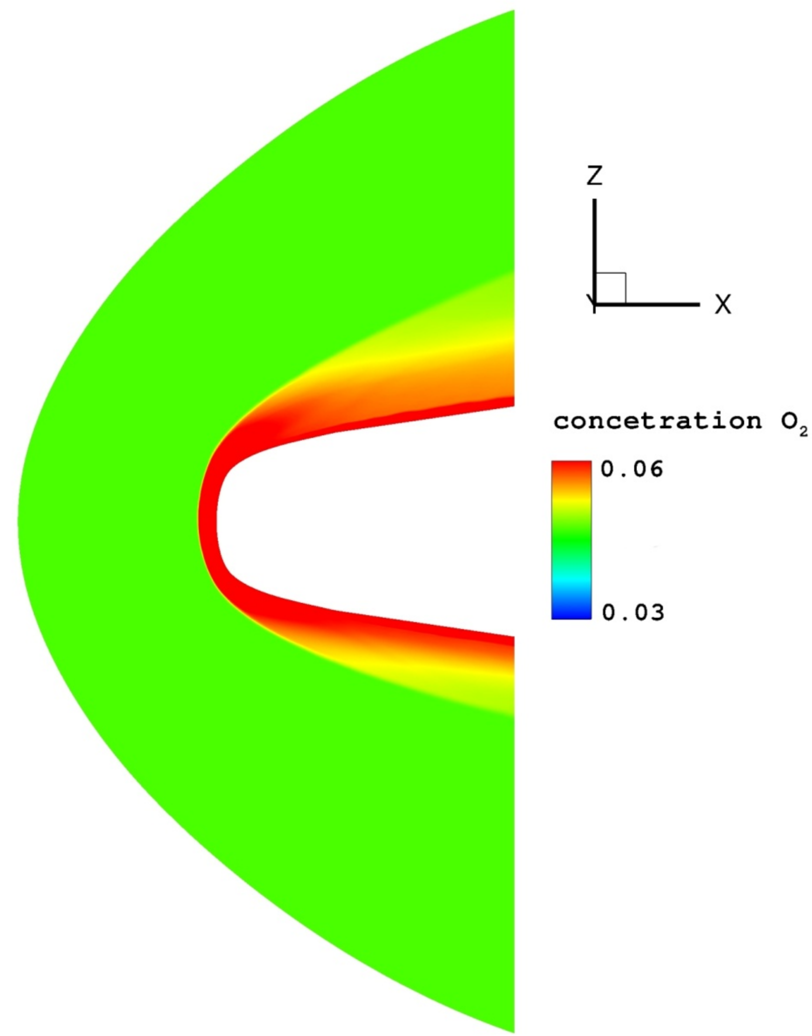

Chemically reacting flow at M = 0.8

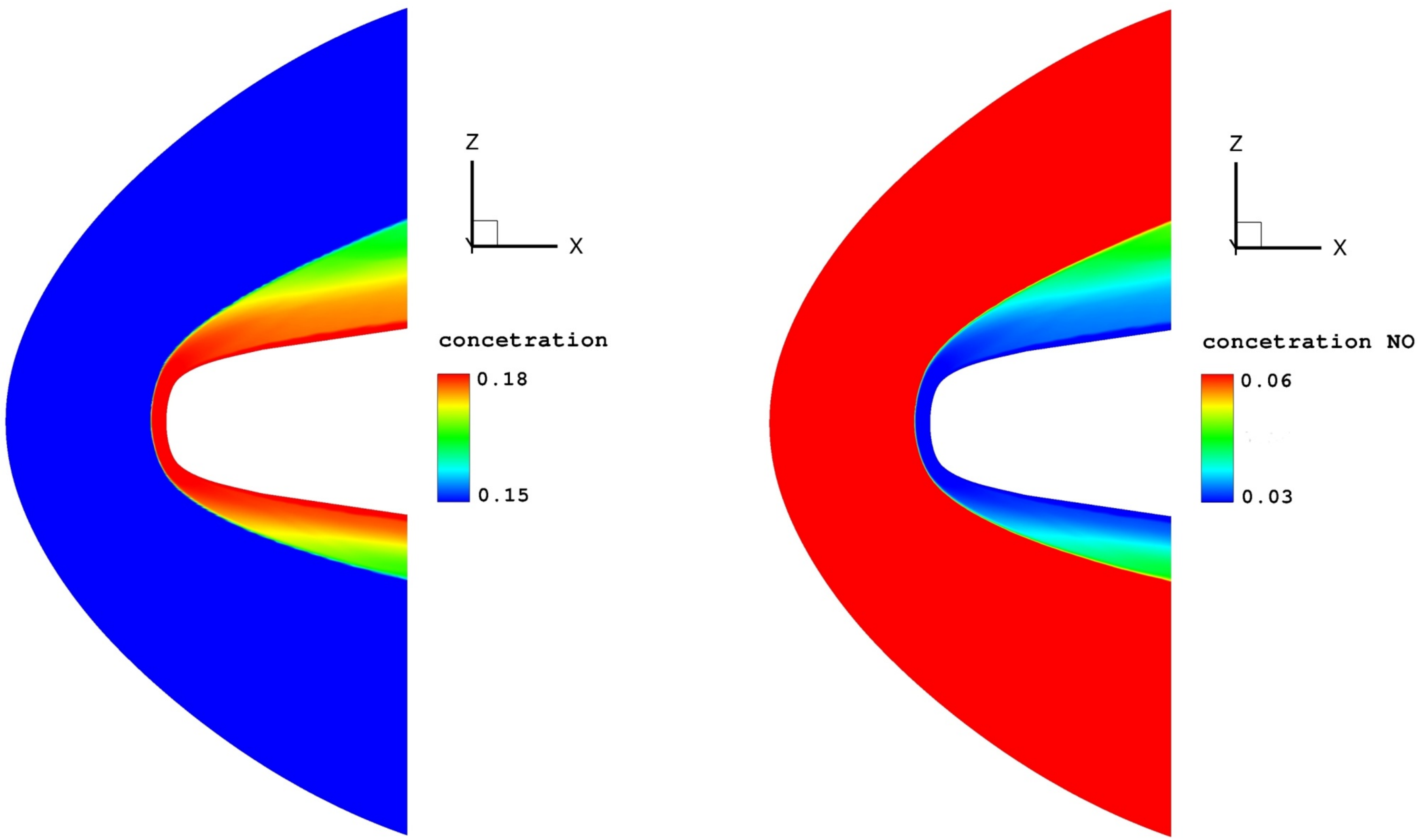

Conclusions

- A unified filtering approach for high order DG discretizations in unstructured three-dimensional meshes was developed

- Filtering is applied as a post processing stage and it is suitable for both implicit and explicit time marching

- Computationally intensive hierarchical limiting of higher order DG discretizations is not required and sub-cell discontinuity resolution is achieved

- Benefits from filtering higher order expansions were found

- Combined dynamic h/p refinement can be applied for problems with discontinuities and embedded smooth but complex flow features to increase efficiency of DG discretizations without compromising numerical accuracy